Chapter 1

Structure-Function Relationship of Heart Valves in Health and Disease

Sotirios Korossis

Additional information is available at the end of the chapter

http://dx.doi.org/10.5772/intechopen.78280

Abstract

The heart valves allow unidirectional and unobstructed passage of blood without regurgitation, trauma to blood elements, thromboembolism, and excessive stress concentrations in the leaflet and supporting tissue. In order to achieve this, the heart valves rely of their unique macroscale anatomy, histoarchitecture and ultrastructural features that allow them to accommodate repetitive changes in shape and dimension throughout the cardiac cycle. This chapter is focused on the structure-function relationship of the heart valves, with particular focus on the aortic and mitral valves, discussing how the biochemical, histoarchitectural and anatomical features influence valvular function during the cardiac cycle and how valvular function dictates valvular architecture and ECM constitution. The chapter examines the structure-function relationship of valvular tissue by correlating its microscale histoarchitecture and biochemical constitution to its mesoscale biomechanics and macroscale function during the cardiac cycle. Moreover, the chapter examines the influence of pathological alterations on the histoarchitectural and biochemical characteristics of the valves on their biomechanical behavior.

Keywords: heart valves, histoarchitecture, biochemistry, biomechanics, structure-function

1. Introduction

Connective tissues comprise a network of interweaving fibers with polysaccharide ground substance immersed in a pool of ionic fluid. Cells are attached to the fibers and are responsible for replenishing the extracellular matrix (ECM) macromolecules and the ground substance that carry out the physical function. The ECM contains three major classes of macromolecules, including structural proteins, such as collagen, elastin and fibrillin, specialized proteins, such

as fibronectin and laminin, and glycosaminoglycans (GAGs) and proteoglycans. The ECM is involved in many normal and pathologic processes, playing an important role in tissue development and pathology, and mechanotransduction of the cells [1]. The ground substance is a hydrophilic gel that fills the spaces between the cells and the ECM. Dense connective tissues contain a small amount of ground substance and the cells are mostly fibroblasts. Loose connective tissues contain significantly more ground substance. Ground substance in normal connective tissues is clear and colorless and its composition varies with the tissue. It has a dense consistency similar to that of maple syrup, due to the presence of GAGs and proteoglycans.

The structure and hence the properties of a tissue are dependent on the chemical and physical nature of its constituents and their relative amounts. For example, nervous tissue consists almost entirely of cells, whereas bone is composed of collagen fibers and calcium phosphate minerals with minute quantities of cells and ground substance. Depending on the functional requirements on a particular tissue, the organization of its ECM macromolecules, cells and ground substance, as well as its resulting mechanical properties, vary. The simplest structure from the point of view of the collagen fibers consists of parallel fibers, as in tendons and ligaments. The 2D and 3D networks of the skin are more complex, whereas the structure of blood vessels and heart valves are the most complex ones. This chapter describes the basic biochemistry and function of the major structural proteins, collagen and elastic fibers, as well as the major GAGs and proteoglycans, present in the ECM of the heart valves, and illustrates their physiological and pathological significance. In addition it examines the structural basis, organization and structure-function relationship of valvular tissue, with particular focus on the aortic and mitral valves, by correlating its microscale histoarchitecture and biochemical constitution to its mesoscale biomechanics. Finally, the chapter examines the influence of pathological alterations, as a result of major valvular disease, on the histoarchitectural, constitutional and biomechanical characteristics of the valves.

2. Structure-function of major ECM proteins of valvular tissue

Proteins are the most abundant organic components of the human body. There are roughly 100,000 different kinds of proteins and they account for about 20% of the total body weight [2]. All proteins contain carbon, hydrogen, oxygen, and nitrogen and in some cases small quantities of sulfur. Proteins are classified according to the function they perform into structural, contractile and transport proteins, buffers, enzymes, antibodies and hormones. From these types, structural proteins such as collagen, elastin and keratin create a 3D framework for the body, providing strength, organization, and support for cells, tissues, and organs. Proteins consist of chains of amino acids, with each amino acid comprising a central carbon atom to which four groups are attached, including a hydrogen atom, an amino group ($–NH_2$), a carboxylic acid group (–COOH) and a variable group, known as an R-group or side chain (**Figure 1a**). The amino and carboxylic acid groups are hydrophilic groups, and amino acids are relatively small, soluble molecules. Depending on the side chain the molecular structure changes drastically, giving each amino acid its individual chemical properties. The simplest R-group is hydrogen, which forms glycine (Gly). Within the physiological pH range, the carboxylic acid groups on many amino acids give up their hydrogen, going from –COOH to $–COO^-$ and getting negatively charged. Two amino acids can be linked by dehydration, which creates a covalent bond between the carboxylic acid group of one amino acid and the amino group

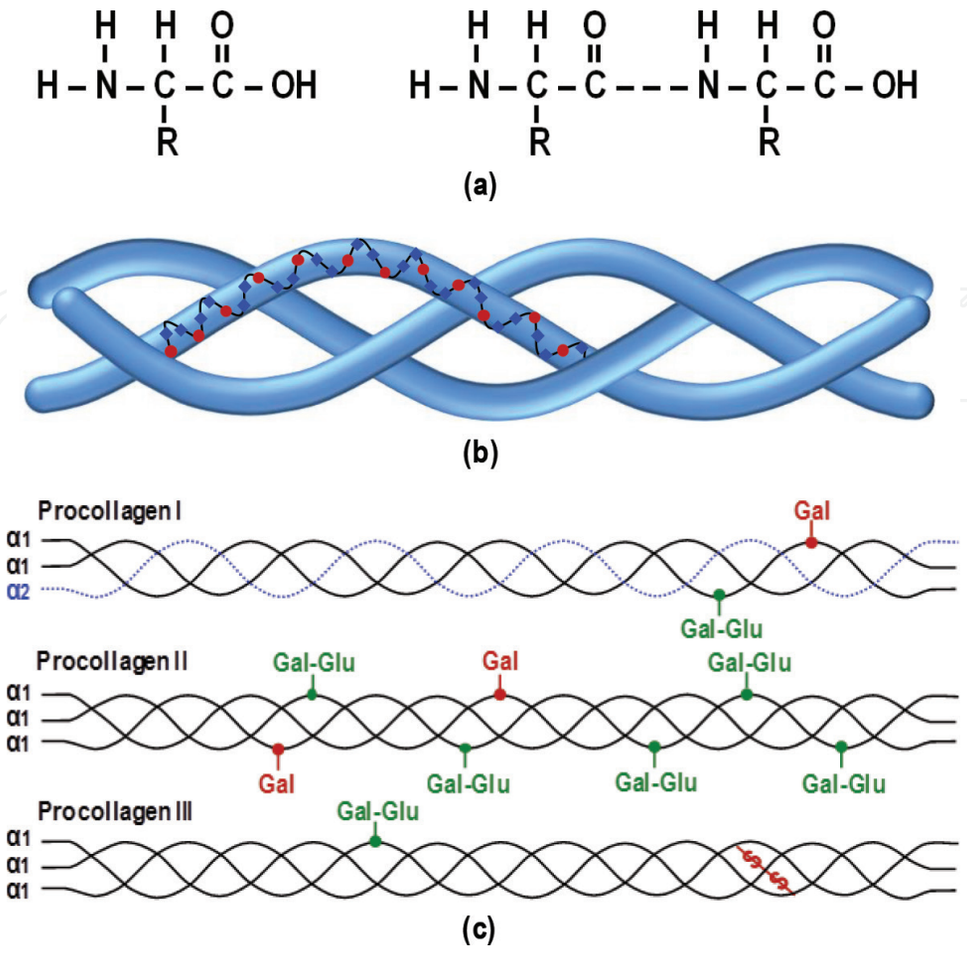

Figure 1. (a) Amino acid structure. (b) Peptide bond formation. (c) Schematic of the collagen triple helix (□ glycine; ♦ other amino acids). (d) Triple helices of procollagen I, II and III; Gal: galactose residue; Glu: glucose residue; redrawn from Nimni (1988) [5].

of the other (**Figure 1b**). Such a bond is known as a peptide bond, and the molecule created dipeptide. The chain can be lengthened by the addition of more amino acids forming polypeptides. Polypeptides containing more than 100 amino acids are usually called proteins. Proteins contain negatively charged amino acids and, therefore, have a net negative charge [2, 3].

Proteins are very versatile and have a variety of different functional properties, which are determined not only by the R-groups on their constituent amino acids, but also by their shape. The primary determinant of shape is the sequence of amino acids (primary structure). The 20 major amino acids present in the human body, can be linked in a high number of combinations, creating proteins that vary in shape and function. Changing the identity of a single amino acid out of 10,000 or more in a protein may significantly alter its functional properties. Further levels of structural complexity include the secondary, tertiary, and quaternary structures. The secondary structure appears as parts of the polypeptide chain, which are bonded together by hydrogen bonding. This usually creates a simple spiral, known as α-helix, or less often a flat pleated sheet, or both. The tertiary structure results primarily from interactions between the polypeptide chain and the surrounding water molecules, and partly from interactions between the R-groups of amino acids in different parts of the molecule. Structural proteins contain several polypeptide chains; each one with its own secondary and tertiary structure. Interactions between these chains determine the quaternary structure of these proteins. The

tertiary and quaternary structure of complex proteins depends not only on their amino acid sequence, but also on the local environmental characteristics, with small changes in the ionic composition, temperature, or pH affecting protein function [1–3].

2.1. Collagen fibers

Collagen is the major insoluble fibrous protein and the basic structural element for soft and hard tissues, supporting elements in the ECM. It is the main load-carrying element giving mechanical integrity and it is present in a variety of structural forms in different tissues. Collagen contains large domains of helical conformation, created by three α-helix polypeptide chains, each containing 1050 amino acids. The individual α-helix chains are left-handed helices with approximately three amino acid residues per turn. The chains are, in turn, coiled together to give a right-handed coiled triple helix (**Figure 1c**), which is the molecular basis of tropocollagen, the precursor of collagen. All collagens have been shown to contain three α-helix chains of similar structure, with each collagen type differentiating its individual properties mainly by incorporating segments that do not follow the triple helix conformation, and fold the collagen molecule into different kinds of three-dimensional structures [3]. The collagen molecule contains a high amount of three amino acids, including Gly, proline (Pro) and hydroxyproline (HYP), and since the latter is unique in collagen (elastin contains minute amount), the collagen content in a tissue can be easily determined by a HYP assay. The characteristic repeating amino acid sequence of the collagen molecule is Gly-X-Y, where X and Y can be any amino acid but are often proline and HYP and less often lysine (Lys) and hydroxylysine (Hyl) [4]. In the amino acid sequence of the collagen molecule every third residue is Gly (**Figure 1c**), whereas proline and HYP follow each other relatively frequently [3, 5, 6]. Hydrogen bonding between the peptide bond NH of Gly and the peptide carbonyl (C=O) group in an adjacent polypeptide (**Figure 1b**), holds the three α-helix peptide chains together in a three-stranded helix, which is formed due to the fixed angle of the C-N peptidyl-Pro or peptidyl-HYP bond [3]. In addition, the α-helixes are cross-linked via Lys, whereas collagen III also contains cysteine (Cys) that can be cross-linked within molecules through disulfide bonds [7]. The side chains of the amino acids of the collagen molecule are highly non-polar and, hence, hydrophobic, seeking the greatest number of contacts with the non-polar side chains of other amino acids. In cases that the hydrophobic contact is destroyed by a solution such as urea, ultrastructural changes are generated in the collagen fibers, such as shrinking [7, 8]. Collagen stability is also affected by the water content in its intra- and inter-chain structure. Specifically, when the water content is decreased the collagen structure gets destabilized, whereas lyophilized collagen also demonstrates decreased solubility [7, 8].

Depending on the source of tissues the collagen chains are different. A characteristic example is demonstrated in **Figure 1d**, which shows the triple helix conformation of three types of collagen, differing in α-helix composition and degree of glycosylation. The amino acid compositions of these chains are listed in **Table 1**. The collagen α-helix chains are synthesized by ribosomes attached to the rough endoplasmic reticulum (ER) as longer precursors called pro-α-helix chains. Subsequently, the pro-α-helix chains undergo a series of covalent modifications in the ER and fold into triple-helical procollagen molecules (**Figure 1d**) before they are released from the cells. Specifically, short non-triple-helical segments at either end (C– and N–terminus) of the pro-α-helix chains, called propeptides and containing Hyl, are covalently linked by disulfide bonds to form

trimers and align the three α-helix chains prior to the triple helix formation in the ER. In addition, specific Pro and Lys residues in the middle of the chains are hydroxylated by hydroxylases, and asparagine-linked oligosaccharides are added to the C-terminal propeptide, whereas galactose (Gal) or galactose-glucose (Gal-Glu) residues are attached to Hyl residues, in a process known as glycosylation [4]. Glycosylation is a common form of post-translational modification of proteins that occurs during processing in the ER and provides intrinsic stabilization of the protein structure and, thus, increases protein half-life and protects them against denaturation or proteolytic degradation [9–11]. The modifications of the α-helices in the ER facilitate their zipping from C- to N-terminus to form stable triple helices in the procollagen molecule. These modifications also allow the binding of the chaperone protein Hsp47 to the procollagen, which has been suggested to further stabilize the helices and/or prevent premature aggregation of the trimers [4]. The modification of the procollagen in the ER is crucial for the subsequent formation of mature collagen,

Amino acid	α1(I)*	α2(I)*	α1(II)*	α1(III)*	Elastin	Microfibril	Tropoelastin
Half-cysteine	Content included in Others				4	48	0
Hydroxyproline					26	151	39
Aspartic Acid	42	44	43	42	21	228	21
Glutamic Acid	73	68	89	71			
Proline	124	113	120	107	595	356	541
Alanine	115	102	103	96			
Valine	21	35	18	14			
Leucine	19	30	26	22			
Methionine	Content included in Others						
Tyrosine							
Phenylalanine							
Isoleucine							
Histidine					13	105	55
Lysine	26	18	15	30			
Arginine	50	50	50	46			
Glycine	333	338	333	350	324	110	334
4-Hydroxyproline	108	93	97	125			
Threonine	16	19	23	13			
Serine	34	30	25	39			
Others**	38	63	72	18			

*I, II and III indicate residues of collagen I, II and III α-helices, respectively.
**Others include 3-hydroxyproline, half-cysteine, methionine, isoleucine, tyrosine, phenylalanine, hydroxylysine, histidine, gal-hydroxylysine, and glc-gal-hydroxylysine.

Table 1. Amino acid residues per 1000 total residues in human collagen [6, 20] and elastin [7].

whereas defects in this process have been reported to have serious consequences. For example, hydroxylation requires the facilitation of vitamin C, and cells deprived of it cannot hydroxylate the procollagen chains sufficiently to form stable triple helices. As a result, non-hydroxylated procollagen chains are degraded within the cell and no collagen fibers can be formed [12]. As a result, in tissues where the turnover (degradation and replacement) of the collagen occurs relatively rapidly, such as in blood vessels and heart valves that experience significant collagen fiber damage due to the repetitive deformation during normal function, the gradual loss of preexisting ECM collagen, which is not supplemented by newly-formed collagen, leads to tissues that are extremely fragile and prone to disintegration [13]. However, in other tissues, such as bone, the turnover of collagen is very low, with collagen molecules reportedly remaining intact for about 10 years [13]. Following the post-translational modification in the ER, the procollagen molecules are transported to the Golgi apparatus, where they are associated laterally to form small bundles, before they are secreted in the extracellular space (exocytosis). Following exocytosis, procollagen peptidases cleave the N-terminal and C-terminal propeptides, transforming the procollagen to tropocollagen molecules, approximately 300 nm long and 1.5 nm in diameter [14]. This allows the tropocollagen molecules to assemble into collagen fibrils by covalent cross-linking between two Lys or Hyl residues at the C-terminus of one tropocollagen molecule with two similar residues at the N-terminus of an adjacent molecule. These cross-links stabilize the packing of the tropocollagen molecules in a quarter-staggered array architecture (**Figure 2a**), generating strong fibrils with a diameter of 50–200 nm and several micrometers long, depending of the species and tissue, with a cross-striated appearance under transmission electron microscopy (**Figure 2b**) [3–6]. The striation has a period (D) of approximately 67 nm, with the lighter part of the striation representing a gap of approximately 0.6D between successive molecules (**Figure 2b**) [6, 15]. The covalent cross-linking between Lys and Hyl residues of adjacent collagen molecules confers significant strength to the collagen fibrils. This type of covalent bonding is only found in collagen and elastin, and its inhibition results in a dramatic reduction of the tensile strength of the fibrils, making tissues fragile and prone to tearing. The extent and type of cross-linking vary from tissue to tissue; in tissues where tensile strength is crucial, collagen is highly cross-linked [13]. Although the alignment of the tropocollagen molecules in the collagen fibril has been idealized as perfectly straight and parallel in **Figure 2a**, in reality they are bent in various degrees, depending on the attachment of water molecules, and have varying spacing between neighboring molecules [6]. Bundles of collagen fibrils form collagen fibers, with diameters ranging between 0.2 and 12 μm, and increasing with age, whereas their length depends on the tissue [16, 17]. Moreover, collagen fibers appear to be crimped (**Figure 2c**), and when the tissue is stretched the amplitude of the crimp decreases [6, 18, 19]. It has been suggested that the crimping of the collagen fibers is generated by the shrinking of the non-collagenous components of the ground substance, which causes collagen fiber buckling [19], whereas enzymatic digestion of the non-collagenous components of the ground substance alters the mechanical properties of the tissue [6].

Collagens are differentiated in terms of their ability to form fibers and organize the fibers into networks. There are at least 20 types of collagen that have been identified and participate in the formation of the ECM of tissues [4]. Among these, types I, II, II, V and XI are fibrillar collagens, with types I, II, III comprising 80–90% of the total collagen in the body [3]. Collagen I is present in almost any tissue, but it predominantly present in bone, dermis, placental membranes, tendons, ligaments, blood vessels and heart valves. Collagen II is mainly located in

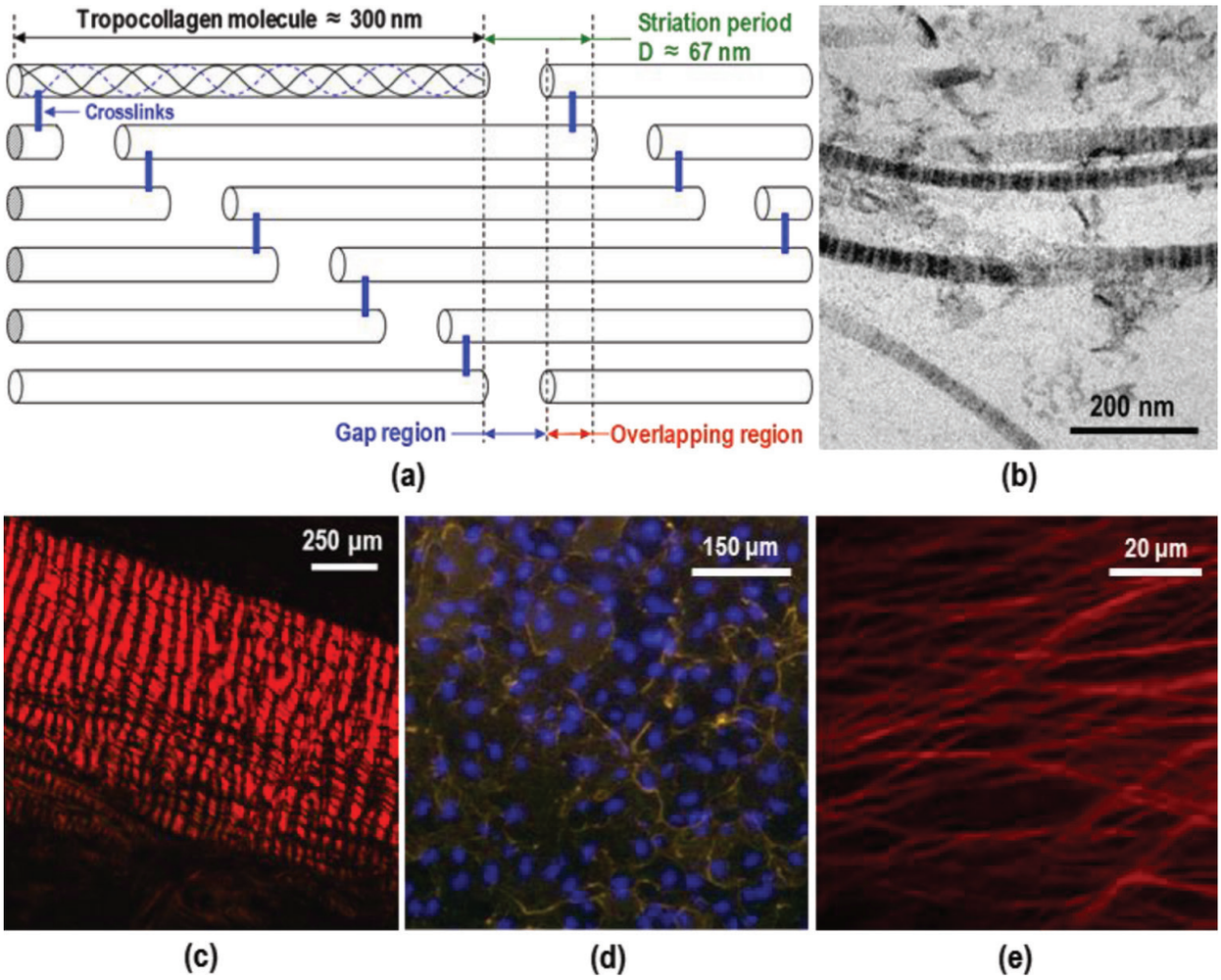

Figure 2. (a) Quarter-staggering of tropocollagen I molecules in collagen fibrils; redrawn from Lodish et al. (2003) [4]. (b) Transmission electron microscopy of the decellularised mitral valve leaflet showing the striations in the collagen I fibrils; adopted with permission from Granados et al. (2017) [68]. (c) Histological section of the anterior mitral valve leaflet stained with sirius red under polarized light, showing the crimping in the collagen I fibers; adopted with permission from Roberts et al. (2016) [18]. (d) Immunofluorescence staining for collagen IV produced by human endothelial cells seeded on culture plastic (yellow/orange: anti-collagen-IV; blue: Hoechst stain for nuclei); adopted with permission from Pflaum et al. (2017) [132]. (e) Two photon microscopy of the atrial surface of the native anterior mitral valve leaflet, showing the elastin in the elastic fiber network.

hyaline cartilage and cartilage-like tissues and the vitreous body of the eye [20]. Similarly to collagen I, collagen III is also quite common in most tissues and represents a major constituent of blood vessels and heart valves, as well as other more distensible connective tissue. Collagen V has a similar distribution to collagen I, but it is a minor constituent in the tissues, whereas collagen XI is found mainly in cartilage and is distributed similarly to collagen II [21]. Collagen VI and IX represent a separate class of collagens that are associated to fibrillar collagens, linking them to each other or to other ECM components. The collagen VI tropocollagen comprises short triple-helical regions of approximately 60 nm long, separated by globular regions of approximately 40 nm long [3]. Collagen VI is common in placental villi [6] and has also been found in many other connective tissues, where it is bound to collagen I fibrils and has been suggested to enable the formation of thicker collagen I fibers [3]. Collagen IX is a proteoglycan in that one of its polypeptide subunits serves as the core protein for a chondroitin

sulfate side chain [6]. The collagen IX molecule comprises two long triple helices connected by a flexible link, on the α2(IX) chain of which the chondroitin sulfate glycosaminoglycan (GAG) chain is covalently linked to [3, 6]. Collagen IX does not assemble into fibrils, due to its interrupted triple-helical conformation. Nevertheless, it is bound along collagen II fibrils at regular intervals, binding them to the GAG- and proteoglycan-rich ECM, and also reportedly contributing to their assembly in collagen II fibers [22]. In addition to collagen IX, collagens XVIII and XV also function as core proteins in proteoglycans.

Collagen IV is a sheet-forming collagen, which is of particular importance for endothelialized and epithelialized tissues, since, together with laminin, is the primary component of all basal laminae, forming their basic two-dimensional fibrous network. Collagen IV, as well as most of the other ECM components that form the basal laminae, is synthesized by the cells that reside on it (**Figure 2d**) [4]. The collagen IV molecule is formed by a 400-nm-long triple helix with large globular domains at the C-terminus and smaller non-collagen ones at the N-terminus, whereas Gly-X-Y sequences of its α-helices are interrupted with segments that do not form a triple helix, and introduce flexible links and flexibility into the molecule [3, 4]. Following exocytosis into the extracellular space, adjacent collagen IV molecules assemble either into groups of 4 molecules by association of their globular N-terminus domains, yielding tetrameric units, or into pairs by association of their globular C-terminus domains, yielding dimeric units [4]. Subsequently, triple-helical regions from several tetrameric and dimeric units associate laterally, similarly to the case of fibril formation in fibrillar collagens, to form branching two-dimensional mesh-like fibrous networks to which other ECM components and adhesion receptors can bind (**Figure 2d**). In addition to the aforementioned types of collagen, other minor classes of collagens include anchoring collagens, such as collagen VII, which connects the basal lamina to the underlying connective tissue, transmembrane collagens, which function as cell adhesion receptors, and host defense collagens, which help the body to recognize and eliminate pathogens [4].

Collagen is encoded by approximately 30 genes, whereas its biosynthetic pathway involves a number of post-translational phases. Owning to this, collagen-related disease most commonly arise from genetic mutations affecting collagen encoding or post-translational modifications, whereas nutritional deficiencies might also affect the post-translational modifications, assembly, or secretion of collagen [1, 13]. Moreover, autoimmune conditions have also been reported to affect collagen fibers, whereas a number of different bacteria and viruses can degrade collagen or interfere with its production pathway [1]. Goodpasture's autoimmune disease causes self-attacking antibodies to bind to the α-helices of collagen IV, setting off an immune response that causes cellular damage [4]. The Ehlers-Danlos syndrome comprises at least 10 types of congenital disorders whose principal features include tissue hyper-extensibility and abnormal fragility. Type IV disorder is the most serious one, especially for the cardiovascular system, which affects collagen III and is associated with spontaneous rupture of arteries or the bowel [1, 13]. Type VI disorder, together with the Bruck syndrome and Menkes disease, are associated with lysyl hydroxylase deficiency, leading to defective cross-linking of collagen and elastin [1, 4, 23], whereas type VIIC disorder causes formation of abnormally thin and irregular collagen fibrils [1]. Moreover, the Alport syndrome is another genetic disorder that alters the C-terminal domain of the tropocollagen IV α-helices and affects the structure of collagen IV fibers, causing structural abnormalities in basal laminae [1, 4].

2.2. Elastic fibers

Elastin is an another structural insoluble fibrous protein, forming a large proportion of the ECM of arteries and veins, especially near the heart, and in other deformable tissues such as ligaments, heart valves, skin, lungs and areolar connective tissue. Elastin is the dominant ECM protein in arteries, contributing about 28–50% of the dry weight of the aorta [13, 23, 24], whereas in elastic ligaments and tendons the elastin content attributes 50 and 4% of the dry weight, respectively [23]. Elastin is the main component of the elastic fibers, which are major insoluble assemblies of the ECM that generate resilience into the tissues by providing a mechanism that permits tissues to deform under load and passively recoil to their original configuration after the load is released, preventing dynamic tissue creep [13, 24–26]. These properties are critical to the function of heart valves, which undergo repeated dynamic cycles of large extension and recoil during opening and closing. In addition to contributing to ECM resilience, the elastic fibers are also an important load-bearing structure, complementing the function of the collagen fibers at the sites where mechanical energy needs to be stored [25]. In particular, the elastic fibers dictate tissue mechanics at low strains before the stiffer collagen fibers are engaged at higher strains [24]. Elastic fibers are the most linearly elastic biosolids known, and are at least five times more extensible than rubber. They are generally twisted or straight with a diameter ranging between about 0.2 and 1.5 μm forming coarse networks (**Figure 2e**) [27]. In dense elastic tissues, such as the arteries, the elastic fibers fuse during development to form flattened co-centric sheets, or elastic laminae, with numerous fenestrations [17, 28, 29].

The elastic fibers are complex structures that comprise several components, with elastin and microfibrils constituting their two major ones [30]. Ultrastructurally, elastic fibers are composed of a homogeneous inner core of laterally packed, thin cross-linked elastin filaments that make up more than 90% of fibers, and an outer fibrillar mantle that consists of microfibrils and surrounds the elastin, accounting for 5–10% of the elastic fibers [23, 25, 26]. The amino acid compositions of these components are given in **Table 1** [7]. The microfibrils are organized into 8–16 nm beaded fibrils and are predominantly made of five distinct proteins, including two fibrillin glycoproteins (fibrillin-1 and fibrillin-2) and two microfibril-associated glycoproteins (MAGP-1 and MAGP-2) [13, 23, 31]. Additional components of the elastic fibers include lysyl oxidase, elastin-binding protein (EBP), proteoglycans, osteopontin, emilin, fibulin-1, and various microfibril-associated proteins [23]. Early development of the elastic fibers involves the assembly of fibrillin molecules in the extracellular space, in enfoldings of the cell surface, into head-to-tail microfibrillar arrays of approximately 160 nm in length that are cross-linked by transglutaminase to form mature beaded microfibrils. Transglutaminase forms γ-glutamyl-e-Lys isopeptide bonds within or between peptide chains [25, 29]. The mature microfibrils, which have a length of approximately 100 nm, form loosely-packed parallel bundles with an one-third-staggered architecture, that have been hypothesized to be stabilized by inter-microfibrillar crosslinking [25]. Non-stretched microfibrils have been reported to have a beaded periodicity of approximately 56 nm, whereas models have predicted up to 8 fibrillin molecules in the microfibril cross-section [25, 27, 31, 32].

Following the formation of the microfibril bundles, intracellularly-produced tropoelastin [33] is gradually deposited among the preformed template of fibrillin-rich microfibrils, until the elastic fibers reach full maturation [7, 23, 25, 26]. Some tissues, even at their mature state, contain bundles of microfibrils devoid of tropoelastin (oxytalan fibers), as well as sites where bundles

of microfibrils are only partially intermixed with tropoelastin (elaunin fibers), and never developed into fully mature elastic fibers [26]. These microfibril states represent interruptions in successive phases of elastic fiber development, indicating that microfibrils can be both progenitors of fully mature elastic fibers in fetal tissues, and independent connective tissue components (oxytalan fibers) [26, 34]. Tropoelastin is the soluble precursor of elastin, which is synthesized by fibroblasts and smooth muscle cells (SMCs) and secreted as a soluble and highly hydrophobic monomer of about 750 amino acids long [13, 24, 35]. Similarly to tropocollagen, tropoelastin contains an abundance of Pro and Gly, but is not glycosylated and contains minute amounts of HYP and no Hyl [13]. Human tropoelastin contains more than 30% Gly, whereas about 75% of its amino acid sequence is made up of just four hydrophobic amino acids, including Gly, valine (Val), alanine (Ala) and Pro [23]. Structurally, tropoelastin comprises two types of alternating segments, including hydrophobic segments and Ala-/Lys-rich α-helical segments, which form cross-links between adjacent molecules [13]. During tropoelastin deposition among the microfibrils, the latter get displaced to the periphery of the growing fiber, allowing the formation of the elastin core by the accumulation of tropoelastin molecules [13, 31]. The accumulated tropoelastin molecules couple covalently to each other by lysyl oxidase-derived cross-links, to form the polymeric elastin, stabilizing the elastin core of the elastic fibers [25, 31]. Lysyl oxidase catalyzes the selective oxidative deamination of Lys residues in tropoelastin, leading to the formation of bi-functional (dehydrolysinonorleucine and allysine aldol), tri-functional (dehydromerodesmosine) and tetra-functional (desmosine and isodesmosine) crosslinks [25]. The resulting cross-linked mature elastin is a very stable and persistent structure that is extremely hydrophobic and insoluble due to the extensive cross-linking at Lys residues [23]. The high stability of elastin has been attributed to the low content of polar amino acid residues, including the anionic Lys, histidine (His) and arginine (Arg), as well as the cationic aspartic acid (Asp) and glutamic acid (Glu) [7].

The elastic recoil generated by the elastic fibers is a critical attribute for tissues that are required to undergo repetitive stretch/relaxation cycles. Tropoelastin is among the most elastic proteins, with a capacity to stretch eight times its resting molecular length (≈20 nm) and recoil without damage, while showing no hysteresis after repeated stretch and relaxation cycles, demonstrating a near perfect spring behavior with minimal energy loss [36, 37]. Atomic force microscopy studies have estimated the Young's modulus of tropoelastin to approximately 3 kPa [37], which is two order of magnitudes smaller (more flexible) than mature cross-linked elastin, estimated between 0.6 and 1.1 MPa [6, 35], four orders of magnitude smaller than microfibrils, estimated between 78 and 96 MPa [38], and six orders of magnitude smaller than mature cross-linked collagen I, estimated between 1 and 1.2 GPa [6, 35]. Given the fact that elastin and elastic fibers are robust structures that effectively last for the lifetime of the organism, studies have suggested that the elastic recoil generated in the elastic fibers cannot be a result of the stressing of the chemical bonds, since this would lead to the fiber deterioration [32]. Several studies have proposed that elastic recoil could be potentially attributed to the change in the number of conformation states of the cross-linked polypeptide chains during stretching and relaxation [6, 7, 13, 39]. Elaborating, under relaxed conditions the cross-linked polypeptide chains adopt a loose random coil conformation, which results in an increased number of different intramolecular conformational states in the chains. Under stretching,

the chains adopt a relatively aligned conformation, limiting their conformational freedom and, thus, decreasing their entropy. Under relaxation, the chains resume their random conformation, increasing the number of different conformational states and, thus, their entropy. This change in the entropy of the cross-linked chains has been suggested to provide the free energy for the elastic recoil [6, 23, 32]. Along these lines, it has been suggested that intramolecular folding of fibrillin molecules at their termini and Pro-rich regions, and at flexible sites between 8-Cys motifs, provides the extension/recoil mechanism of microfibrils [25, 27]. Similarly, cross-linked mature elastin has been suggested to derive its high elasticity from the cross-linking of Lys residues into desmosine, isodesmosine, and lysinonorleucine [7].

In contrast to collagens that can be encoded by large gene families, there is only one gene (ELN) that is responsible for synthesizing tropoelastin [40, 41]. Tropoelastin is mainly synthesized *in utero* and early childhood, whereas by middle-age only a small amount of this molecule is produced [23, 42]. Owing to this, elastin is the longest lasting protein in the body, with a half-life of approximately 74 years [23, 43]. However, in the event of elastin damage due to acquired disease or aging, the low levels of tropoelastin produced mean that elastic fibers cannot be repaired sufficiently. Along these lines, loss of elasticity, due to degradative changes in elastic fibers, is a major contributing factor in connective tissue aging, and aortic aneurysm development [23, 25, 44, 45]. Elastic fiber degradation has also been reported to occur in atherosclerosis, with atherosclerotic vessels presenting increased stiffness, together with calcium and lipid accumulation in the elastic fibers [23, 46].

In the case of genetic disorders, mutations in the genes of the components of the elastic fibers have been associated with congenital disorders in elastic fiber-rich connective tissues. Specifically, Marfan syndrome and other overlapping disorders, such as MASS (mitral valve prolapse, aortic dilation, and skin/skeletal manifestations) syndrome, and autosomal TAAD (thoracic aortic aneurysms and dissections) [47], termed fibrillinopathies [48], have been associated with fibrillin-1 mutations, leading to increased fragmentation of the elastic fibers that, in turn, lead to life-threatening cardiovascular disease and severe skeletal and ocular defects [13, 25, 38]. Progressive aortic valve root dilation, aortic dissection and rupture, and aortic or mitral valve regurgitation are the most serious conditions associated with Marfan syndrome, with a 90% mortality rate in these patients. Neonatal patients with Marfan syndrome die perinatally from congestive heart failure and valvular deficiency [38].

Increased fragmentation of the elastic fibers has also been reported in cutis laxa and Menkes disease, the latter of which is associated with tortuous blood vessels and abnormalities in other tissues [23]. Moreover, the pseudoxanthoma elasticum and Buschke-Ollendorff syndromes have been associated with fragmentation, clumping and calcification of elastic fibers, leading to cardiovascular defects [23, 25]. Elastin mutations that cause elastin deficiency have been reported to cause reduced elastin content and disruption in the architecture of aorta and heart valves in Williams syndrome and supravalvular stenosis (SVAS) [23, 25, 29]. Elastin has been reported to induce actin stress fiber organization and inhibit SMC proliferation [24], indicating that apart from its structural role, elastin has a role in arterial morphogenesis [23]. Owing to this, reduction in the elastin content causes narrowing of the aorta and other arteries, and SVAS [23, 25], due to the excessive proliferation of SMCs [13, 24].

3. Glycosaminoglycans and proteoglycans

GAGs (also termed mucopolysaccharides) are the most abundant unbranched heteropolysaccharides in the body, composed of repeating disaccharide units [1]. Disaccharides are formed by two simple sugars (monosaccharides; basic units of carbohydrates), which are joined by dehydration synthesis. Polysaccharide chains are large, stiff and complex molecules that exist in tissues as highly viscous materials that interact with proteins and readily bind both water and cations. The GAGs derive their name from the fact that one of the two sugars in their repeating disaccharide unit is always an amino sugar, either N-acetylglucosamine (N-acetyl-D-glucosamine; GlcNAc) or N-acetylgalactosamine (N-acetyl-D-galactosamine; GalNAc) [1, 7, 13]. The other of the two sugars is usually either an uronic acid (glucuronic acid or iduronic acid) or D-galactose [1, 4, 13], whereas one or both of the sugars contain at least one anionic group (carboxyl or sulfate) [4], rendering GAGs highly negatively charged [13]. Owing to the relatively high stiffness and hydrophilicity of the polysaccharide chains, GAGs form extended conformations with a large volume to mass ratio, forming hydrated gels even at very low concentrations, and imparting high viscosity and, thus, low compressibility, to the ECM. The gel-forming character of the GAGs is due to their high negative charge that attracts cations, especially Na^+, which causes large osmotic inflow of water into the ECM, creating a swelling pressure that enables the ECM to withstand compressive loads [1, 13]. The GAG gels can form with varying pore size and charge density, and it has been suggested that they act as selective sieves to regulate molecule and cell traffic according to their size and charge [13]. Although GAGs constitute less than 10% of the weight of the fibrous proteins in the ECM of connective tissues, their high volume to weight ratio and gel-forming ability enables them to fill most of the extracellular space, providing mechanical support to the tissue [7, 13], as well as lubrication between tissue (joints) and elastic and collagen fibers [2, 6].

Depending on the type of the repeating disaccharide unit, type of linkage between the sugars, and number and location of sulfate groups, GAGs are classified into four groups, including (i) hyaluronic acid, (ii) heparan sulfate and heparin, (iii) keratan sulfates (I and II), and (iv) chondroitin sulfates (chondroitin 4-sulfate and chondroitin 6-sulfate) and dermatan sulfate (**Table 2**) [1, 4, 13]. Hyaluronic acid is the simplest GAG and the only one that it does not contain any sulfate or attach covalently to proteins as a proteoglycan. However, it does form complexes with proteoglycans in the ECM, non-covalently [7]. All other GAGs contain sulfate groups, either as O-esters or as N-sulfate (in heparin and heparan sulfate) [1]. Heparin is a hyper-sulfated form of heparan sulfate that produced by mast cells and is an important anticoagulant that can activate the antithrombin III clotting inhibitor in plasma [1, 4]. It can also bind to the lipoprotein lipase, which is a membrane-associated enzyme present in capillary walls that hydrolyzes triglycerides to fatty acids, causing its release into the circulation [1, 4]. Hyaluronic acid is abundant in embryonic tissues and has been suggested to play an important role in facilitating cell migration during morphogenesis and wound repair, whereas high concentrations of hyaluronic acid, as well as chondroitin sulfates, in tissues contribute to their compressibility. Keratan sulfates and dermatan sulfate lie between collagen fibrils and play a critical role in their alignment. Heparan sulfate is associated with cell membranes and has been suggested to act as a receptor mediating in cell growth and cell-cell and cell-ECM communication [1]. In adult tissues, GAGs have a slow turnover, with half-lives between days and weeks [1].

With the exception of hyaluronic acid, all GAGs are found covalently linked to a polypeptide chain, or core protein, forming proteoglycans that are synthesized by most cell types [4]. Proteoglycans is a diverse group of highly glycosylated glycoproteins, which are distinguishable from other glycoproteins by the nature, quantity, and arrangement of their sugar side chains [13]. Proteoglycans feature at least one GAG side chain, whereas their carbohydrate content can reach up to 95% of their weight [1, 13]. On the other hand, the carbohydrate content of glycoproteins is between 1 and 60% of their weight, an is present in the form of numerous relatively short, branched oligosaccharide chains [2, 13]. Proteoglycans have the potential of almost limitless heterogeneity [13], differentiating in the type of core protein, number and types of GAG chains, and number of disaccharide modifications by sulfate groups [1, 4, 13]. Some of the most common proteoglycans that have been characterized are listed in **Table 2**. Similarly to other proteins, the core proteins of proteoglycans are synthesized by ribosomes attached to the ER, and translocated into the lumen of the ER. Subsequently, the core protein is transported to the Golgi apparatus where it is glycosylated [1, 2]. During glycosylation, the GAGs are linked to their core proteins in one of three different modes. The first two modes involve the formation of O-glycosidic bonds between the hydroxyl side chains of serine (Ser) residues in the core protein and a xylose (Xyl) residue, which is unique to proteoglycans, or between Ser residues in the core protein and GalNAc residues in the GAG chain (keratan sulfate II). In the first case, two Gal residues are subsequently added to the Xyl residue sequentially, forming a link trisaccharide (-Gal-Gal-Xyl-) that serves as a polysaccharide growth primer, followed by further linear growth of the GAG on the Gal terminal of the link trisaccharide (**Figure 3**). The third mode involves the formation of N-glycosylamine bonds, as found in N-linked glycoproteins, between the amide nitrogen of asparagine (Asn) residues in the core protein and the GlcNAc residues of the GAG chains [4, 13]. Subsequently, the polysaccharide chains are often modified in the Golgi apparatus by the covalent linkage of

<table>
<tr><th>GAG</th><th>Localization</th><th colspan="3">Small Proteoglycans</th><th colspan="3">Large Proteoglycans</th></tr>
<tr><td>Hyaluronic acid</td><td>Synovial fluid, vitreous humor, loose connective tissue, heart valves, blood vessels</td><td colspan="3">-</td><td colspan="3">-</td></tr>
<tr><td>Heparan sulfate</td><td>Basal laminae, cell surface, blood vessels, liver, skin</td><td colspan="2"></td><td rowspan="3">Testican, Syndecan-1</td><td colspan="2"></td><td rowspan="3">Perlecan</td></tr>
<tr><td>Chondroitin sulfate</td><td>Heart valves, blood vessels, basal laminae, cartilage, bone, cell surface</td><td>Bikunin</td><td rowspan="2">Decorin, Biglycan, Betaglycan</td><td>Neurocan, Aggrecan, Brevican</td><td rowspan="2">Versican</td></tr>
<tr><td>Dermatan sulfate</td><td>Heart valves, blood vessels, skin</td><td></td><td></td><td></td></tr>
<tr><td>Keratan sulfate</td><td>Cornea, bone, cartilage</td><td colspan="3">Fibromodulin, Lumican</td><td colspan="3">Aggrecan (with Chondroitin sulfate)</td></tr>
</table>

Table 2. Prevalent localization of different GAG types and their associated proteoglycans.

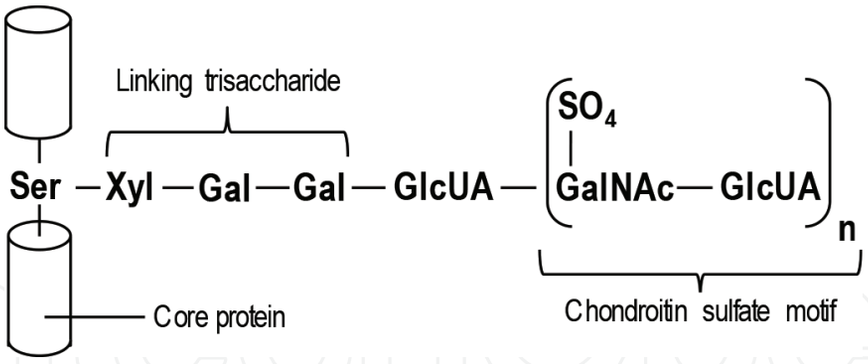

Figure 3. Biosynthesis of proteoglycans, showing the case of the linking of chondroitin sulfate chains to their core protein. Ser: serine residue; Gal: galactose residue; GlcUA: glucuronic acid residue; Xyl: xylose residue. Modified from Alberts et al. (2014) [13] and Lodish et al. (2003) [4].

small molecules, such as sulfate groups onto GalNAc and other moieties and the epimerization of GlcUA to IdUA residues. Following glycosylation, the completed proteoglycan is then exported in secretory vesicles to the ECM [1, 4, 13].

In the extracellular space, proteoglycans bind various secreted signal molecules, such as growth factors, enhancing or inhibiting their signaling activity [13]. They also bind to other types of secreted proteins, including proteases and protease inhibitors, regulating their activities [1, 4]. Moreover, GAGs and proteoglycans can associate to each other to form big aggregates. Such a case is the aggrecan proteoglycans, which comprise chondroitin sulfate and keratan sulfate, and assemble with hyaluronic acid. GAGs and proteoglycans also associate with fibrous proteins, such as collagen and basal laminae, creating extremely complex structures. Such a proteoglycan is decorin, which comprises chondroitin sulfate and dermatan sulfate, and binds to collagen fibrils, aiding in collagen fiber formation. Decorin deficiency has been reported to lead to reduced tensile strength in tissues [13, 49–52]. Another proteoglycan of this type is perlecan, which is major proteoglycan of basal laminae, consisting of heparan sulfate and chondroitin sulfate chains linked to a large multi-domain core protein. Perlecan is incorporated in the basal laminae by binding to both laminin and collagen IV, connecting the two networks, and defining the structure and function of basal laminae. Owing to its multi-domain components, perlecan can also cross-link cell surface molecules to ECM components [4]. In addition to proteoglycans that fully reside in the extracellular space, some proteoglycans form integral components of the cell membranes by having their core protein spanning or attached to the lipid bilayer of the cell membrane. Such proteoglycans are the syndecans, which comprise three chondroitin sulfate and heparan sulfate chains and are expressed by many cell types, including epithelial cells and fibroblasts [13, 53–55]. Syndecans bind to ECM collagens and other ECM proteins such as the fibronectins, anchoring cells to the ECM, while interacting with the intracellular actin cytoskeleton [4].

The importance of GAGs and proteoglycans is emphasized by the severe developmental defects that can occur when specific proteoglycans are inactivated by mutation. A number of congenital enzyme deficiencies have been linked to GAG metabolic disorders (mucopolysaccharidoses) [13]. Among mucopolysaccharidoses, the Hurler [56–59] and Hunter [60–62] syndromes are the most widely studied. Mucopolysaccharidoses are associated with mutations in the gene encoding lysosomal hydrolases, including endoglycosidases and exoglycosidases,

which are enzymes involved in GAG degradation [56, 57, 62]. Absence or malfunctioning of lysosomal hydrolases lead to GAG accumulation in various tissues, including liver, spleen, bone, skin, and central nervous system [1, 60, 61]. Moreover, severe congenital deficiency in dermatan sulfate synthesis leads to a short stature, prematurely aged appearance, and generalized defects in the skin, joints, muscles, and bones of individuals [13]. GAGs and proteoglycans have also been associated with major diseases, such as cancer and atherosclerosis, and aging. The intima of arterial walls contains, among others, dermatan sulfate proteoglycans, which are synthesized by arterial SMCs and bind plasma low-density lipoproteins that are involved in atherosclerotic plaque development. Since atherosclerotic lesions feature increased proliferation of SMCs, the dermatan sulfate content is increased in these sites, suggesting a potential role of this GAG in atherosclerotic plaque development [63]. Moreover, the amount of chondroitin sulfate diminishes with age, whereas the amounts of keratan sulfate and hyaluronic acid increase. These changes may contribute to conditions, such as osteoarthritis, and other degenerative diseases, as well as the characteristic changes in aged skin in the elderly [1, 2].

4. Structure and constituents of normal heart valves

Depending on the functional requirements for a particular tissue, the organization of fibers, cells and other ECM macromolecules in the tissue and, thus, the mechanical properties of the tissue vary. The simplest structure from the point of view of the collagen fibers consists of parallel fibers as in tendons and ligaments. The 2D and 3D networks of the skin are more complex, whereas the structures of aortic, pulmonary, mitral and tricuspid valves in the heart are the most complex ones. The structure of the heart valves is adapted to allow unidirectional and unobstructed passage of blood without regurgitation, trauma to blood elements, thromboembolism, and excessive stress concentrations in the valve leaflets and supporting tissue. The cellular and extracellular elements of normal valves accommodate repetitive changes in shape and dimension throughout the cardiac cycle. They provide effective stress transfer to the annulus and adjacent tissue, and mediate functional remodeling and repair of injury caused by the large repetitive deformations. The aortic and pulmonary valves comprise three similar-size leaflets, and are located between the left ventricle and aorta, and the right ventricle and pulmonary artery, respectively. Their leaflets resemble half-moons and, thus, they are referred to as semilunar (SL) valves. The mitral valve (MV) is located between the left ventricle and left atrium, and comprises two noticeably different leaflets that resemble a bishop's miter when they are closed. The tricuspid valve is located between the right ventricle and right atrium, and comprises three leaflets. Owing to their location between the atria and the ventricles, the mitral and tricuspid valves are referred to as the atrioventricular (AV) valves. In addition to their leaflets, the AV valves also comprise fan-shaped tendinous chord (chordae tendinae) that link the AV valve leaflets to protrusions on the ventricular wall, the papillary muscles, and act similarly to the parachute chords, preventing the AV valve leaflets to prolapse into the atria when they are fully closed.

The aortic and pulmonary valve leaflets open against the aorta and pulmonary artery, respectively, during ventricular systole, whereas the mitral and tricuspid valve leaflets open against the myocardial wall of the right and left ventricle, respectively, during ventricular diastole. The semilunar valves close during ventricular diastole and the atrioventricular valves

during systole. All four valves close rapidly and completely under minimal reverse pressure, stretching to maintain full competence during diastole. During these opening and closing movements, the valve leaflets withstand cyclic strains as high as 50%, whereas despite the pressure difference across the closed valves, which imposes large load on their leaflets, leaflet prolapse is prevented by large coaptation of the leaflets, reaching up to 40% of their surfaces [18, 64–68]. Even though each of the four heart valves has its own individual unique anatomical, structural and constitutional features that are adapted to their specific localization and function, they share common structural, constitutional and functional features. Moreover, the aortic and mitral valves are the ones most prone to disease, since they reside in the high pressure environment of the left ventricle. Owing to these, the discussion in the following paragraphs is focused on the aortic and mitral valves, as representatives of the SL and AV valves, respectively. Moreover, the discussion will focus on valve leaflets, since these are the most structurally complex and constitutionally diverse components of the heart valves.

The heart valve leaflets are layered with a highly specialized ECM, which provides the basis for normal valve function. Two types of cells are present, including a layer of endothelial cells (ECs) that covers the luminal surface of the leaflets and a deep layer of interstitial cells (VICs) that consists of SMCs and fibroblasts, which replenish and remodel the valvular ECM [69]. The EC layer is continuous with the luminal surface of the atrium and ventricle, in the case of the AV valves, and ventricle and adjacent artery (pulmonary artery or aorta) in the case of the SL valves. The aortic valve leaflets comprise three distinct layers, including the fibrosa, spongiosa and ventricularis, each enriched in a different ECM component (**Figure 4a–c**, **e**). The MV leaflets present a slightly different architecture, with four layers instead of three, including a ventricularis, a fibrosa, a spongiosa and an atrialis layer (**Figure 4c**, **e**). Within these layers, the structural elements are arranged in a methodical orientation, leading to leaflet properties that are highly anisotropic. Several structural features enable the semilunar and atrioventricular leaflets to be extremely soft and pliable when unloaded and inextensible when high transvalvular pressure is applied during the time the valves are fully closed [18, 65, 70, 71]. In the case of the aortic valve, the fibrosa layer faces the outflow (aorta side) of the valve, whereas in the case of the MV the fibrosa lies below a ventricularis layer, which faces the outflow (left ventricle side) of the valve. The fibrosa in both valve types is the primary structural layer and major load bearing layer that offers the mechanical integrity of the valve leaflets [72]. The predominant constituent of the fibrosa are large amounts of highly-aligned collagen I fibers (**Figure 4c**), which are organized into large bundles and are predominantly aligned along the circumferential direction of the leaflets. The collagen I fibers of the fibrosa are surrounded by glycosaminoglycans and proteoglycans, as well as a network of elastic fibers, which maintains the microstructure of the valve leaflet during unloading [73]. This directionality of the collagen fibers results in aortic and MV leaflet structures that are considerably stiffer along their circumferential direction than their radial [18, 67, 73]. Moreover, folds in the collagen layer of the fibrosa generate a macroscopically visible corrugations on the surface of the leaflets when they are un-stretched (**Figure 4a**).

The ventricularis layer of the aortic valve is equivalent to the atrialis of the MV in function and organization, with both facing the inflow of the valves. Although these layers are less organized than the fibrosa, they still contain significant amounts of collagen I (**Figure 4c**) and radially aligned elastic fibers (**Figure 4d**). However, because the collagen is not oriented in any

http://dx.doi.org/10.5772/intechopen.78280

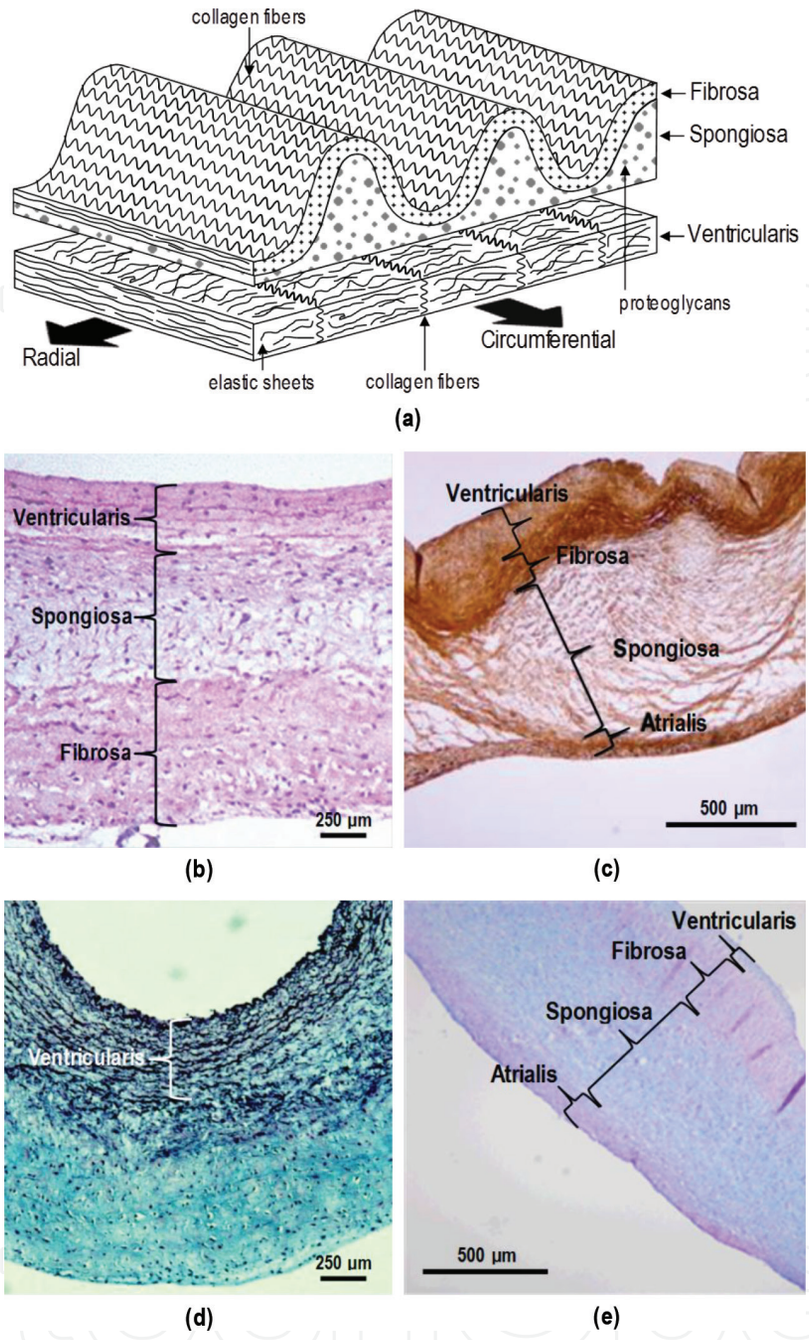

Figure 4. (a) Trilaminar leaflet structure of semilunar valves, showing the fibrosa, spongiosa and ventricularis layers, together with their major constituents. Note the macroscopically visible corrugations of the fibrosa layer. (b) H & E histological staining of the aortic valve leaflet (radial direction). ECM proteins were stained pink/light purple; cells were stained deep/purple. (c) Immunohistochemical staining against collagen I of the mitral valve posterior leaflet (radial direction). Collagen I was stained brown. (d) Miller's elastic histological staining of the aortic valve leaflet (radial direction). Elastic fibers were stained deep blue/black. (e) Alcian blue/PAS histological staining of the mitral valve anterior leaflet (radial direction), showing the ventricularis, fibrosa, spongiosa and atrialis layers; dark blue: cell nuclei; blue: acid mucosubstances (GAGs) and proteoglycans; magenta: Neutral polysaccharides.

specific direction, they tend to be more flexible than the fibrosa. The elastic fibers of the aortic valve ventricularis and MV atrialis extend when the leaflets stretch to enlarge the coaptation area, but recoil to make the leaflet smaller in the open valve phase. The ventricularis of the MV

is similar in structure and constituents to the MV atrialis and aortic valve ventricularis, with loosely arranged collagen fibers and radially-aligned elastic fibers (**Figure 5a**). The spongiosa layer is located between the fibrosa and ventricularis of the aortic valve, and between the fibrosa and atrialis in the MV. This layer is primarily composed of water, GAGs and proteoglycans (**Figure 4e**), but also contains loosely arranged collagens and elastin, which connect the fibrosa and ventricularis (or atrialis) together. Shear stresses caused by the differential movements of the leaflet layers and the shock of the valve closure are dissipated in the ground substance of the spongiosa, whose hydrophilic GAGs and proteoglycans absorb water and swell to form a deformable gel [69]. The thickness of the leaflet layers varies from the attachment site (basal area) at the valvular annulus to the free edge of the leaflets [72, 73]. At the basal area, the fibrosa comprises the thickest layer, becoming thinner and gradually overtaken by the spongiosa towards the free edge of the leaflets (**Figure 5b**). The spongiosa is the main component of both the SL and AV valve leaflets at their free edge, providing a natural shock-absorption mechanism along the coaptation region of the leaflets that dissipates the shocks of valve closure [67, 73]. The thickest regions of the leaflets, especially close to their basal regions, also feature venules and arterioles, which facilitate supplementary oxygen and nutrient transport in regions where simple diffusion is not sufficient for cell nourishment (**Figure 5a** and **b**) [18, 66, 72, 74].

During the cardiac cycle, the SL and AV valve leaflets undergo significant changes in their macroscale and microscale architectural configuration. When the valves are fully open, the gross corrugations of the fibrosa, which are caused by folds in the collagen fiber layer, produce a visible surface wrinkling (**Figure 5c**), which disappears when the leaflets are fully extended when the valve is fully closed and loaded under the peak transvalvular pressure (**Figure 5d**). During valve closing, the corrugations of the fibrosa expand along the radial direction, which is accompanied by radial stretching of the radially-aligned elastic fibers of the SL ventricularis (or MV atrialis) layer, permitting initial increase in dimension with minimal stress. Further stretching of the leaflets causes uncrimping of the collagen fibers along the circumferential direction. When the valve is fully closed, the collagen-layer folds are fully extended and the corrugations in the fibrosa are fully flattened along the radial direction, whereas collagen fibers are uncrimped along the circumferential direction. These changes produce stiffening of the leaflets, preventing their exaggerated sagging and ensuring optimal coaptation with the adjacent leaflets when the valve is fully closed [64, 69]. On the other hand, the stretching of the elastic fibers provides the energy that is necessary for the elastic recoil of the leaflets to their upstretched configuration when the valve is fully open. Moreover, the multilayered structure of the valve leaflets has been reported to contribute to the low flexural rigidity of the leaflets when the valves are fully open, possibly also due to interlayer slippage, that allows their passive interaction with the surrounding blood [75]. The multilayered leaflet structure also provides additional support during valve closure and coaptation, assisting the extended collagen fibers to generate a stiffened leaflet structure that prevents exaggerated sagging under the high transvalvular pressure [73].

In addition to collagen I, collagens III, IV, V and VI have also been identified in the heart valves [72, 76–78]. Even though these collagens are expressed in varying concentrations in the four valves, their localization and distribution has been shown to be similar in all valves. Apart from the fibrosa layer, were it is has a dominant presence, collagen I is expressed throughout the SL and AV valve leaflets (**Figure 4c**), whereas collagen III is most evident in

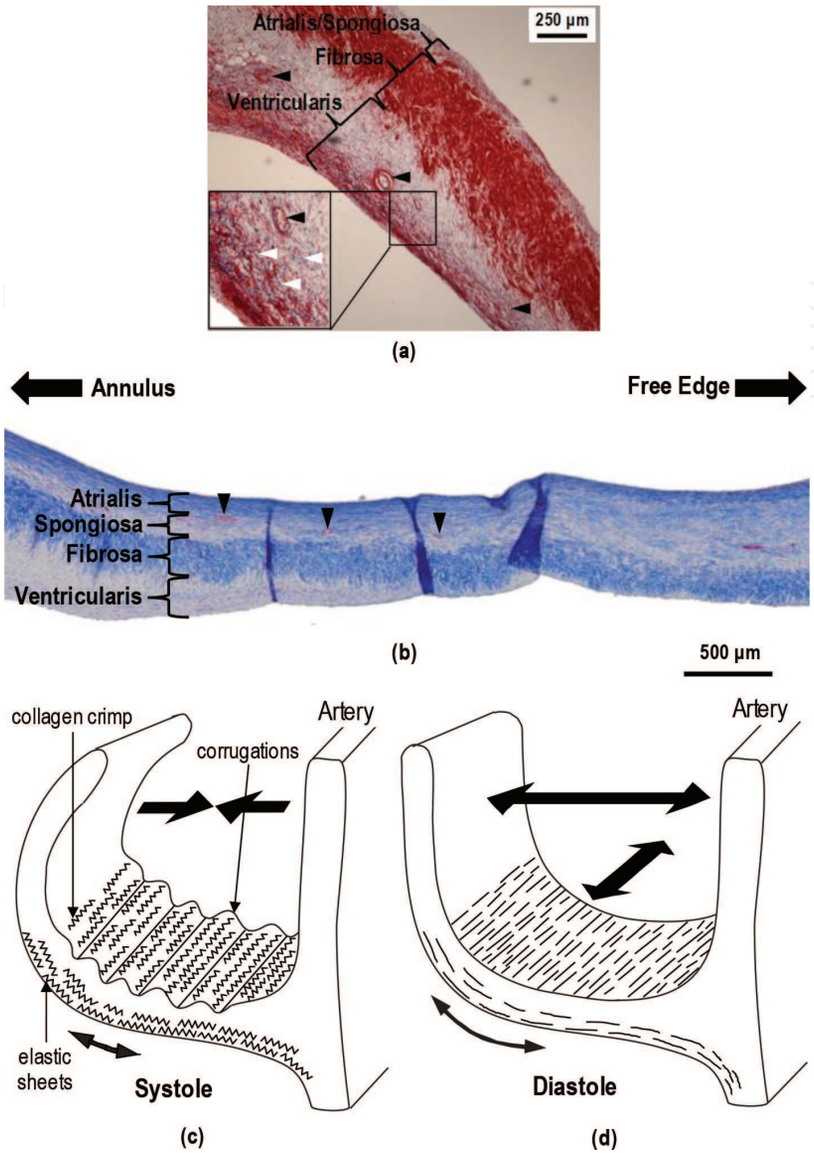

Figure 5. (a) Radial histological section of the basal region of the posterior MV leaflet stained with Miller's elastic and sirius red (red: collagen; blue/black: elastin). ▷ indicates elastic fibers; ▶ indicates blood vessels. Note the dominance of the fibrosa and ventricularis layers in the expense of the spongiosa layer in the basal region. (b) Radial histological section of the posterior MV leaflet stained with Masson's Trichrome stain (blue/black: cell nuclei; red: cytoplasm; blue: collagen). ▶ indicates blood vessels. Note the increase in the thickness of the spongiosa layer and the decrease in the thickness of the fibrosa layer towards the free edge of the leaflet. Adopted with permission from Roberts et al. (2016) [18]. (c, d) leaflet configuration and architecture of semilunar valves during peak systole (c; fully open) and peak diastole (d; fully closed). Redrawn and modified from Schoen (1999) [64].

the less-dense regions of the leaflets, such as the spongiosa [76]. Collagen IV has been shown to be localized in the basal lamina of the leaflets and collagen V to be predominantly distributed around interstitial cells. Collagen VI has been shown to form distinct structures within the fibrosa, surrounding the dense collagen I fibers of this layer [76]. The total collagen content in normal valve leaflets is approximately 50–63% (dry tissue weight ratio) [68, 71, 79, 80], and the elastin content is approximately 10–11% (dry tissue weight ratio), depending on the valve type (**Table 3**) [78, 80–83]. Previous studies have reported the relative percentages of

	Content			
Constituent	**Aortic Leaflet**	**Pulmonary Leaflet**	**Mitral Leaflet**	**Mitral Chordae**
Hydroxyproline (μm/mg dry tissue)	71.6±26.1 (H) [79]	70.7±6.2 (P) [71]	88.2±3.9 (P) [68]	88.6±7.1 (P) [68]
Total collagens (μm/mg dry tissue)	511.2±186.3(H) [79]	504.8±44.3 (P) [71]	629.7±17.8 (P) [68]	632.6±50.7 (P) [68]
Sulfated GAGs (μm/mg dry tissue)	11.4±0.4 (H) [79]	20.2±0.6 (P) [71]	26.8±3.5 (P) [68]	15.5±5.4(H)* [78]
Elastin (% of dry tissue weight)	11.2±1.0 (H)** [81]	N.A.	10.0±17.8 (H) * [78]	9.7±2.1 (H) * [78]

The results indicate mean ± 95% confidence intervals, or mean ± standard deviation (*), or means ± standard error (**). H: Human; P: porcine; N.A.: not available. Numbers in brackets indicate source document.

Table 3. Hydroxyproline, collagen, sulfated GAG and elastin content of normal heart valves.

collagen I, III, and V in normal human MV leaflets to be approximately 74, 24 and 2% of the total collagen content, respectively, whereas collagen IV and VI were below the detection limit of the technique used in those studies [72, 77]. A similar study by Lis et al. [78] reported a collagen I to collagen III ratio of 2.4 and 2.7 for human MV leaflets and chordae, respectively.

Three major GAGs have been identified in varying concentrations in heart valves, including chondroitin sulfate, dermatan sulfate and hyaluronic acid, together with decorin, biglycan and versican, which are chondroitin and dermatan sulfate proteoglycans [51, 84, 85]. The total content of sulfated GAGs (chondroitin and dermatan sulfate) in normal heart valves has been reported to range between 11 and 27% (dry tissue weight ratio), depending on valve type and site (**Table 3**) [68, 71, 78, 79]. Hyaluronic acid is the most abundant GAG in normal heart valves, accounting for up to half of the total leaflet GAG content, with chondroitin and dermatan sulfate accounting for about a quarter of the total GAG content of the leaflet each [86]. The relative percentages reported for normal human MV leaflets were 49, 25 and 23% of the total GAG content, for hyaluronic acid, chondroitin sulfate and dermatan sulfate, respectively, with the remaining 3% attributed to hyper-sulfated chondroitin/dermatan sulfate. In the case of the normal MV chordae, the corresponding percentages have been reported to be 24 (hyaluronic acid), 26 (chondroitin sulfate), 43 (dermatan sulfate) and 7% (hyper-sulfated chondroitin/dermatan sulfate) [84–86]. Moreover, differences in the absolute and relative GAG contents have been reported for different regions of the valves, subjected to different modes of loading during the cardiac cycle. Specifically, regions of the valves that are predominantly subjected to tensile loading, such as the leaflet belly and chordae (in the case of the AV valves), present a reduced overall GAG content compared to regions such as the free edge of the valve leaflets, which are predominantly subjected to compressive loading during coaptation with the other valve leaflets when the valve is fully closed. In addition, the regions that are predominantly subjected to tensile loading present significantly increased levels of chondroitin and dermatan sulfate compared to hyaluronic acid [85].

5. Physiological behavior of heart valves under loading

The ultrastructural histoarchitecture of the valvular tissue and the interaction of its collagen fibers with its non-collagenous components form the basis of the mechanical properties of heart valves. Similarly to other biological tissues that are subjected to high deformation and loading, collagen and elastic fibers act synergistically in heart valves to provide valvular tissue with strength and elasticity, respectively, which are required for their efficient function. The strength and stiffness of the collagen fibers prevent fracture of the valvular components when they are subjected to the peak transvalvular pressure during the time the valves are fully closed. The tensile strength of collagen is approximately 120 MPa, which is only one order of magnitude lower than high tensile steel (about 1110 MPa) and an elastic modulus of about 1.2 GPa, which confers substantial stiffness (**Table 4**) [35, 87]. However they stretch only minimally (about 13%) [35, 88]. On the other hand, elastic fibers are the most extensible biosolids known with very low modulus of approximately 0.3–1.1 MPa (**Table 4**) and capable of reaching failure strains in excess of 150%. However, elastic fibers demonstrate a low tensile strength of approximately 2 MPa, which limits their load-bearing capacity [35].

During the cardiac cycle, valvular tissue deforms to relative large strains, exhibiting non-linear stress-strain behavior. A typical stress-strain behavior for SL valve leaflet tissue within its physiological range is shown in **Figure 6a**. The graph describes the behavior of SL valve leaflets

Material	Young's modulus / Elastic phase modulus (MPa)	Collagen phase modulus (MPa)	Source
Tropoelastin	0.003	-	[37]
Microfibrils	78-96		[38]
Mature cross-linked elastin	0.3-1.1	-	[6, 35]
Collagen 1 fibrils		95.5	[75]
Mature cross-linked collagen 1	-	$1.0 - 1.2 \times 10^3$	[6, 35]
Aortic leaflet (C)	0.07	39.0	[65, 66]*
Aortic leaflet (R)	0.04	2.1	
Pulmonary leaflet (C)	0.76	15.3	[71]*
Pulmonary leaflet (R)	0.34	1.2	
Mitral leaflet (C)	0.02	10.2	[68]*
Mitral leaflet (R)	0.02	2.1	
Mitral chordae	0.10	113.7	

C: Circumferential direction, R: radial direction.
*Data obtained under uniaxial tensile testing.

Table 4. Indicative low-strain and high-strain modulus of valvular tissue and constituents.

from peak systole, when the SL valves are fully open, to peak diastole, when the SL valves are fully closed and loaded by the maximum transvalvular pressure. The graph also shows the contributions of the elastic and collagen fibers towards the overall behavior of the tissue and can be better comprehended in conjunction with **Figure 5c** and **d**. This type of stress-strain behavior has three distinct phases [65]. During the first phase (elastic phase), the leaflet offers little resistance to elongation since force transmission and load bearing is provided mainly by the elastic fibers. During this phase the collagen layer in the fibrosa unfolds and the collagen fibrils change their angular distribution [75]. Owing to these, the collagen fibers have minimal contribution to force transmission, resulting in a stress-strain response for this phase that is characterized by a low slope (low modulus). In the elastic phase the leaflet tissue behaves almost as an elastic solid with the stress increasing linearly with the strain. Under further loading, the leaflet enters the transition phase, during which the collagen fibers uncrimp and gradually align and uncoil, increasing their contribution to the force transmission. In the collagen phase, all the collagen fibers are uncoiled (recruited) and the load is entirely borne by them. Further extension in the collagen fibers occurs by extrafibrillar (between molecules) and interfibrillar shear in the fibers, as well as molecular distortion [35]. Interfibrillar shear has been reported to be dependent on the amount of proteoglycans associated with the surface of the fibrils, which influences the extent of GAG association and electrostatic interactions between the fibrils and the surrounding ECM [35]. The slope of the stress-strain curve for the collagen phase is steep (high modulus) and almost constant, reflecting the material properties of the collagen fibers, which allow limited elongation to fracture [89]. Although the collagen phase of the leaflet continues well beyond the physiological range before failure, corresponding to the reserve strength of the collagen fibers, after peak systole the valve starts opening again and the stress is relieved whilst the leaflets recoil back to their original shape/size at peak systole. A similar non-linear stress-strain profile can be observed for the case of the leaflets and chordae of the AV valve during their closing phase from peak diastole to peak systole. Moreover, experimental studies have indicated that the stress-strain response of valve leaflets were independent of strain rate [75]. The Young's modulus of different valvular tissue constituents, together with the elastic and collagen phase slopes of pulmonary and aortic valve leaflets, and MV leaflets and chordae, are listed in **Table 4**.

Similarly to other biological tissues, the stress-strain behavior of valvular tissue also demonstrates viscoelastic behavior. Generally, viscoelasticity is manifested by a number of different features, including hysteresis, preconditioning, stress relaxation and creep. Viscoelasticity is a fundamental characteristic of biological materials, which exhibit both viscous and elastic behavior, depending on their constitution, temperature and the time over which the tissue is observed. Under cyclic loading (**Figure 6b**), valvular tissue exhibits a hysteresis loop (a phase lag) between loading and successive unloading. The area under the loading curve represents the energy stored during the extension of the tissue, whereas the area under the unloading curve represents the energy recovered during the recoil of the tissue back to its unloaded state. The hysteresis is the area between the loading and unloading curves of the stress-strain response and it is proportional to the mechanical energy dissipated. The hysteresis provides a measure of the energy storage efficiency of the tissue, with the larger the hysteresis the less efficient is the energy storage capacity of the tissue during loading and the less energy is returned to the system on unloading [90, 91]. Both collagen and elastic fibers do not show significant hysteresis, which makes them efficient in energy storage and able to provide the

necessary energy for rapid retraction of the valve leaflets during opening [35, 75, 91]. The energy storage capacity of the elastic fibers has been linked the high entropy of the elastin molecules. In the case of collagen, the intrafibrillar and interfibrillar shear, and molecular distortion that occur during the collagen fiber stretching has been suggested to contribute to the elastic energy storage [35]. Overall, valve leaflets have been reported to demonstrate a relatively low hysteresis of approximately 12% (in the case of the MV), which is independent of the strain rate [75].

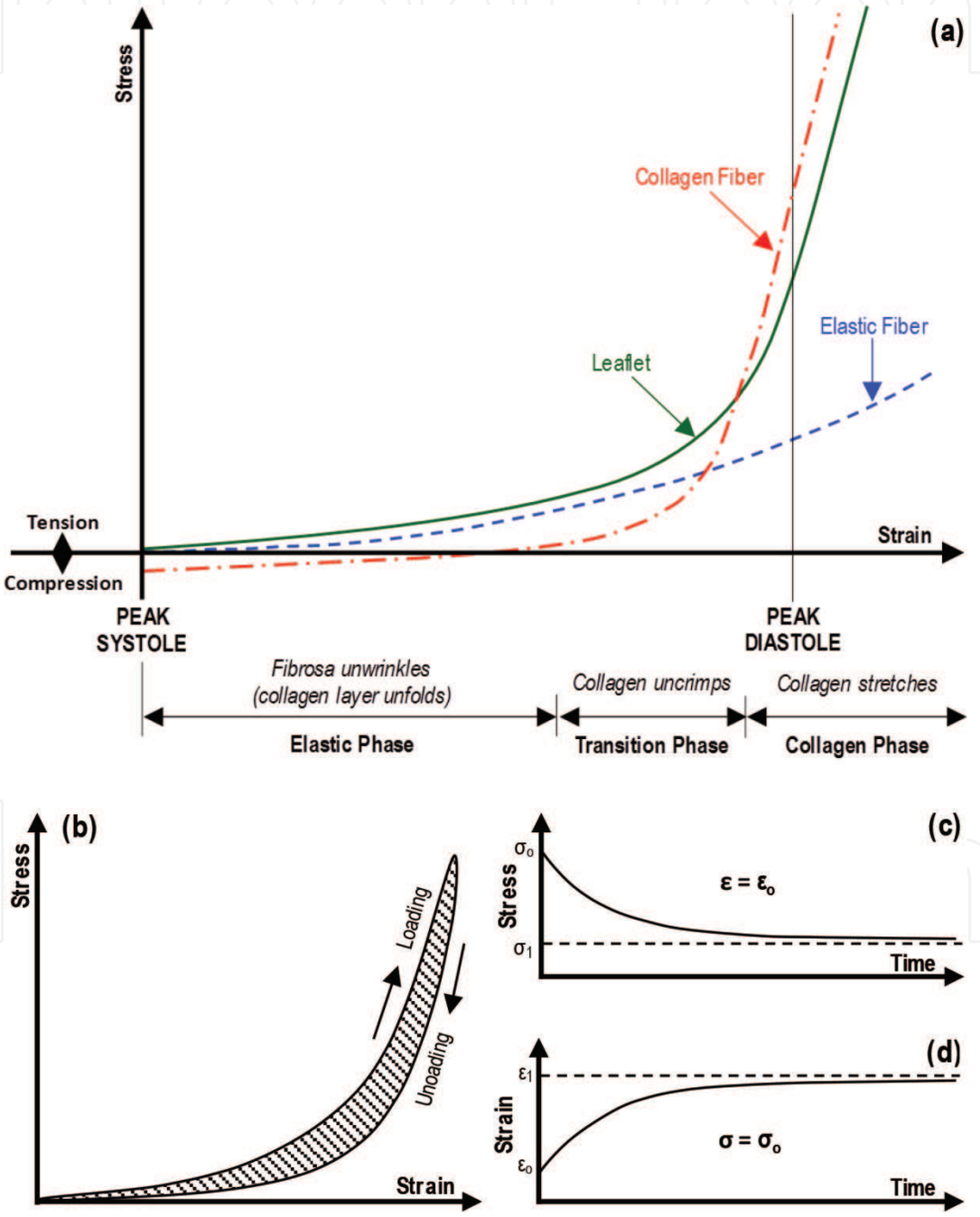

Figure 6. (a) Structure-property relation of SL valve leaflets within physiological ranges of stress and strain. Redrawn and modified from Schoen (1999) [64]. (b) Successive loading and unloading of biological tissue, showing the hysteresis loop (hashed area). (c) Stress relaxation under constant strain. (d) Creep under constant stress.

Following altered loading conditions, valvular tissue reorganizes itself to compensate for the altered mechanical stress, demonstrating an initial period of adjustment in its stress-strain behavior under cyclic loading [75]. This adjustment is manifested by an increased hysteresis loop, which subsequently decreases, tending to a steady state after a number of loading/unloading cycles. Once this steady state is reached, no further change occurs in the stress-strain behavior, unless the loading routine is changed again. This period of adjustment after a large disturbance is called preconditioning and occurs due to internal changes in the structure of the tissue during cycling [6]. The viscoelastic feature of stress relaxation is manifested by the reduction of the stress generated in the tissue over time under constant strain (**Figure 6c**). Specifically, if the tissue is suddenly loaded to an initial stress σ_o and its length held constant, the stress relaxes asymptotically to a limiting value σ_1 following an exponential decay. Creep is the counterpart of stress relaxation in the sense that the tissue is loaded to a strain ε_o and the stress is held constant. Under these conditions the specimen continuous to deform asymptotically to a limiting value ε_1 (**Figure 6d**) [92]. Studies have reported that valve leaflets exhibit significant stress relaxation, but negligible creep over time, suggesting that they behave more like anisotropic quasi-elastic materials rather than viscoelastic materials. This behavior suggests that valve leaflets exhibit a load-locking behavior under maintained loading conditions that enables them to withstand high loading without any time-dependent deformation effects [75].

The degrees of non-linear stress-strain behavior, hysteresis, preconditioning, stress relaxation and creep are different for different tissues, depending on the type and amount of their individual constituents [6, 92]. Along these lines, the variability in the biomechanical properties between the different valves and valve components (**Table 4**) is predominantly due to the different fractions and organization of the major ECM constituents, including collagen fibers, elastic fibers, GAGs and proteoglycans, present in the different valves and valve components. These constitutional and organizational variations, which are dictated by the specific hemodynamic and biomechanical environment that the valves reside in, bequeath high directional and regional histoarchitectural and biomechanical anisotropy to the valvular tissue, assisting the heart valves to perform their specific function in the four different sites of the heart.

6. Structural, constitutional and biomechanical alterations in pathological heart valves

Heart valve surgery for repairing or replacing dysfunctional represents the second most common major heart operation in the western world [93]. In the US alone, approximately 5 million patients are diagnosed annually with heart valve disease [75, 94, 95]. Any one of the heart valves can potentially demonstrated valve disease; however, the aortic and mitral valves are most prone to disease, predominantly due to the higher stress that are subjected to and generated by the high pressure environment of the left heart [75]. Various conditions in isolation or in combination can cause valve dysfunction, including inflammation, degenerative valve disease, calcification, rheumatic or infective endocarditis, myocardial infarction and congenital defects, such as bicuspid aortic valve (BAV), MV prolapse (MVP), isolated anomalous lobar pulmonary veins and silent patent ductus arteriosus [96, 97]. Valve disease is manifested by

disruptions and alterations in the ECM histoarchitecture and constitution, disruptions in the distribution and organization of the EC and VIC populations, and malformation of the heart valves, which can render them stenotic and/or regurgitant [74, 75]. Moreover, several ECM gene mutations have been linked to valve disease, including fibrillin 1 gene mutations, which have been associated with BAVs and MVP, and elastic fiber component gene mutations also associated with MVP (Williams and Marfan syndromes) [98–100]. MVP and pulmonary valve stenosis have also been linked to collagen III and tenascin X gene mutations [98], whereas Notch1 gene mutations have been associated with BAV development and early calcification [101, 102]. Several studies have suggested that the abnormal organization of the ECM induced by these mutations may lead to abnormal VIC signaling and subsequent dysregulation of ECM synthesis [98, 103–105].

BAVs in the most common form of congenital valve disease, affecting 1–2% of the general population and eventually leading to aortic valve stenosis or regurgitation, infective endocarditis, and aortic dilation and/or dissection later in life [80, 97, 98, 106, 107]. Stenotic BAVs explanted from pediatric patients have been reported to exhibit excessive ECM production and disorganization, and VIC disarray without calcification. [98]. Specifically, the valve leaflets demonstrated loss of the typical trilaminar structure of the normal aortic valve leaflets, with disorganized, fragmented and abnormally oriented collagen and elastic fibers, increased proteoglycan presence throughout the leaflets, leaflet thickening, and large areas relatively void of cells. Moreover, elastin content was decreased, whereas collagen and proteoglycan content were substantially increased [75, 98]. The abnormalities in BAV histoarchitecture, constitution and anatomy, have been show to affect leaflet kinematics and stress distribution in computational studies, suggesting that early occurrence of regurgitation or stenosis might strictly depend on those abnormalities [107]. Alterations in the mechanical loading of the heart valves, due to abnormalities in histoarchitecture, constitution and anatomy, induce tissue remodeling though abnormal VIC mechanotransduction, which can lead to further valvular disease and dysfunction. Several studies have characterized VIC response against alterations in the biomechanical environment, and demonstrated a clear link between abnormal VIC stimulation, valvular tissue deformations and disease development and progression, highlighting the fundamental role of the mechanical environment on the mechanobiology of VICs [108–111]. As a result, BAVs are highly susceptible to calcification in later life, due to an induced osteoblastic VIC phenotype and subsequent matrix mineralization [80, 112]. Calcification causes valvular tissue to become thicker and stiffer (representative of a higher modulus), which eventually leads to valve stenosis and inevitable valve replacement [75].

Calcified aortic valve disease (CAVD) is not restricted to BAVs alone. CAVD is a slow, progressive, multifactorial disorder that is frequently driven by aging and the obesity-associated metabolic syndrome, and affects 25–30% of the population aged over 65 years old [75, 84, 100, 105, 113, 114]. Initially, the disease in manifested by mild leaflet thickening of the leaflets alongside with increase in the proteoglycan and hyaluronic acid content, which progressively become more severe and lead to impaired leaflet motion, valvular tissue adaptation and stenosis, [75, 84]. In spite of the leaflet thickening, studies have indicated that there is little change in the mechanical properties of the valve at the early stages of the disease [75]. Although this makes the condition asymptomatic at its initial phases, 10% of the patients develop severe symptoms within 10 years

of the initial diagnosis, and require immediate AV replacement [115]. Accumulating evidence suggests that apart from the upregulation of certain cellular pathways that can activate VIC transdifferentiation into osteogenic phenotype and promote osteogenic ECM remodeling, several non-cellular mechanisms, such as epitaxial calcification, can also induce calcium deposition in heart valves [116]. Calcific deposits in CAVD typically occur in regions of high stress concentration [117], highlighting the importance of mechanical factors in valve calcification, and initiate on the outflow surface of the leaflets [80, 106, 118]. It has been hypothesized that valvular ECs may regulate VIC function, and that the initiation of calcific deposits on the outflow, rather than the inflow, surface of the leaflets is due to differences in the hemodynamic microenvironment on the two sides of the leaflet. Elaborating, the different hemodynamic environments generate different mechanical forces that induce different phenotypic modulations on the ECs on the opposing sides. This, in turn, causes variations in the regulation of VIC function [80, 119]. Moreover, accumulating evidence suggests that CAVD shares common features with atherosclerosis, particularly the early accumulation of low-density lipoproteins (LDL), possibly by proteoglycan retention, and the attraction of inflammatory cells by hyaluronic acid, in the early stages of both pathologies [84]. These commonalities have led to the suggestion that there might be an regulatory mechanism of CAVD, similar to that in arterial atherosclerosis [84, 106, 120]. It has been suggested that a potential mediator of the hemodynamics-induced differential EC modulation might be Kruppel-like factor 2 (KLF2) [80]. KLF2 is a shear-stress-regulated transcription factor that is selectively induced in ECs localized in arterial regions that are protected from atherosclerosis [121]. Along these lines, ECs exposed to the same shear stress as the inflow surface of the aortic valve leaflets, demonstrated upregulation of KLF2 relatively to ECs exposed to shear stress levels equivalent to the outflow surface the aortic leaflets [80]. Moreover, it has also been suggested that the initiation of calcific deposits on the outflow surface of the leaflets might be due to the presence of nucleation sites, which provide the starting point for calcium nodule formation [75].

MVP is another common form of congenital valve disease that affects more than 2% of the general population, and it is the most common indication for surgical MV repair or replacement. MVP refers to the displacement of one (unileaflet MVP) or both (bileaflet MVP) MV leaflets into the left atrium during systole [80]. MVP is not apparent at birth and it usually remains asymptomatic till late adulthood [75, 80]. The condition is characterized by gross changes in the MV components, including thickening, enlargement and hooding of the leaflets, annular dilation, and elongated and/or ruptured chordae [86, 122]. The underlying pathology of MVP is myxomatous degeneration, which is defined by the abnormal accumulation of mucopolysaccharides. The pathology engulfs a number of processes, including diminishing of the fibrosa and thickening of the spongiosa layer of the leaflets, increased cellularity in the spongiosa, deposition of randomly orientated collagens, accumulation of GAG- and proteoglycan-rich myxomatous material in the leaflets and chordae, fragmentation of collagen and elastic fibers, and production of abundant matrix metalloproteases [80, 86, 123, 124]. These changes in the histoarchitecture and constitution lead to the biomechanical weakening of the MV components, which ultimately leads to mitral regurgitation, thromboembolism, heart failure and atrial fibrillation [75, 80]. Myxomatous MVs have been reported to demonstrate a lower strength, increased extensibility and decreased modulus compared to normal MVs in both the leaflets and chordae [86, 125, 126]. Myxomatous degeneration has also been reported to affect the biomechanical integrity of the chordae more that it does in the case of the leaflets [125, 126]. This finding is in accord with clinical reports that have indicated that most cases of myxomatous mitral regurgitation

involve chordal elongation and/or rupture rather than isolated leaflet prolapse due to annular dilation [86, 122]. In terms of constitution, human myxomatous MV leaflets and chordae have been reported to contain 3–9% more water and 2.4–7% more collagen compared to the normal tissues. In addition, the myxomatous leaflets and chordae contained 30–150% more GAGs compared to the normal tissues, with chordae from unileaflet prolapsing valves demonstrating 62% more GAGs than chordae from bileaflet ones [86]. The alteration in the histoarchitecture and biochemical constitution is an attribute of the altered biosynthetic response of the VICs [80]. This leads to the pathological remodeling of the myxomatous valves, which coupled with their normal wear induced during the cyclic loading, leads to the deterioration of their mechanical integrity. As discussed above, abnormalities in histoarchitecture and constitution cause alterations in the mechanical loading generated in the heart valves and, thus, abnormal VIC mechanotransduction. Indeed, VICs have been shown to respond to mechanical strain *in vitro* and modulate their biosynthetic and ECM-degradation activity. Under cyclic straining, VICs, isolated from porcine MV leaflets and chordae, produced upregulation of GAGs, with chordal VICs responding more rapidly to the cyclic strain than leaflet VICs [127, 128]. Moreover, studies with human MV explants have reported that during MVP development, healthy quiescent VICs undergo a phenotypic activation though the upregulation of the BMP4-mediated pathway [75, 129, 130]. BMP4 is an osteogenic morphogen that, together with BMP2, have been shown to be present in ossified valves [131]. BMP4 is also a potent inducer of collagen and proteoglycan synthesis, and matrix mineralization [75].

Acknowledgements

This work was supported by the People Programme (Marie Curie Actions) of the EU 7th Framework Programme FP7/2007–2013/ under the REA Grant Agreement Number 317512, and the German Research Foundation through the Cluster of Excellence REBIRTH (From Regenerative Biology to Reconstructive Therapy; EXC 62). The author is also funded by the German Centre for Lung Research (DZL) BREATH (Biomedical Research in End-stage and Obstructive Lung Disease Hannover) (DZL: 82DZL00201), and the German Research Foundation through a Project Grant (348028075).

Conflict of interest

The author has no conflict of interest to report.

Author details

Sotirios Korossis

Address all correspondence to: korossis.sotirios@mh-hannover.de

Hannover Medical School, Hannover, Germany

References

[1] Murray RK, Keeley FW. The extracellular matrix. In: Murray RK, Granner DK, Mayes PA, Rodwell VW, editors. Harper's Illustrated Biochemistry. 26th ed. New York, NY: McGraw Hill; 2003. pp. 535-555

[2] Martini FH, Nath JL, Bartholomew EF. Fundamentals of Anatomy & Physiology. 9th ed. Harlow, UK: Pearson (Verlag); 2011. pp. 1-1264

[3] Lodish H, Berk A, Zipursky L, Matsudaira P, Baltimore D. Molecular Cell Biology. 4th ed. Proto-Oncogenes and Tumor-Suppressor; 2000; Section 24.2

[4] Lodish H, Arnold B, Matsudaira P, Kaiser CA, Krieger M. Molecular cell biology. 5th ed. New York, NY: W. H. Freeman; 2003. 973p

[5] Nimni ME. The cross-linking and structure modification of the collagen matrix in the design of cardiovascular prosthesis. Journal of Cardiac Surgery. 1988;**3**(4):523-533

[6] Fung Y-C. Biomechanics. New York, NY: Springer New York; 1993

[7] Park J, Lakes RS. Biomaterials: An introduction. In: Biomaterials: An Introduction. 3rd ed. New York, NY: Springer-Verlag; 2007. pp. 1-561

[8] Lee JH, Khang G, Lee HB. Blood leak-proof porous vascular grafts. In: Wise DL, Trantolo DJ, Lewandrowski K-U, Gresser JD, Cattaneo MV, editors. Biomaterials Engineering and Devices: Human Applications: Volume 1: Fundamentals and Vascular and Carrier Applications Basis. Totowa, NJ: Humana Press; 2000. pp. 161-179

[9] Shental-Bechor D, Levy Y. Folding of glycoproteins: Toward understanding the biophysics of the glycosylation code. Current Opinion in Structural Biology. 2009;**19**(5):524-533

[10] Sarkar A, Wintrode PL. Effects of glycosylation on the stability and flexibility of a metastable protein: The human serpin α1-antitrypsin. International Journal of Mass Spectrometry. 2011;**302**(1-3):69-75

[11] Varki A. Biological roles of oligosaccharides: All of the theories are correct. Glycobiology. 1993;**3**(2):97-130

[12] Gelse K, Pöschl E, Aigner T. Collagens—structure, function, and biosynthesis. Advanced Drug Delivery Reviews. 2003;**55**:1531-1546

[13] Alberts B, Johnson A, Lewis J, Morgan D, Raff M, Roberts K, et al. Molecular Biology of the Cell. 6th ed. Vol. 6. New York, NY: Garland Science; 2014. p. 1465

[14] Canelón SP, Wallace JM. β-Aminopropionitrile-induced reduction in enzymatic cross-linking causes in vitro changes in collagen morphology and molecular composition. PLoS One. 2016;**11**(11)

[15] Viidik A. Thermal contraction-relaxation and dissolution of rat tail tendon collagen in different ages. Aktuelle Gerontologie. 1977;**7**(9):493-498

[16] de Souza RR. Aging of myocardial collagen. Biogerontology 2002;**3**(3):325-335

[17] Ushiki T. Collagen fibers, reticular fibers and elastic fibers. A comprehensive understanding from a morphological viewpoint. Archives of Histology and Cytology. 2002;**65**(2): 109-126

[18] Roberts N, Morticelli L, Jin Z, Ingham E, Korossis S. Regional biomechanical and histological characterization of the mitral valve apparatus: Implications for mitral repair strategies. Journal of Biomechanics. 2016;**49**(12):2491-2501

[19] Dale WC, Baer E, Keller A, Kohn RR. On the ultrastructure of mammalian tendon. Experientia. 1972;**28**(11):1293-1295

[20] Kühn K. The classical collagens: Types I, II, and III. In: Mayne R, Burgeson RE, editors. Structure and Function of Collagen Types. Orlando: Academic Press; 1987. pp. 1-42

[21] van der Rest M, Garrone R. Collagen family of proteins. The FASEB Journal. 1991;**5**(13): 2814-2823

[22] Olsen OH, Samuelsen MR, Petersen SB, Norskov L. Excitations in three-dimensional models of alpha-helix structures in proteins. Physical Review A. 1988;**38**(11):5856-5866

[23] Vrhovski B, Weiss AS. Biochemistry of tropoelastin. European Journal of Biochemistry. 1998;**258**(1):1-18

[24] Patel A, Fine B, Sandig M, Mequanint K. Elastin biosynthesis: The missing link in tissue-engineered blood vessels. Cardiovascular Research. 2006;**71**(1):40-49

[25] Kielty CM, Sherratt MJ, Shuttleworth CA. Elastic fibres. Journal of Cell Science. 2002; **115**(Pt 14):2817-2828

[26] Montes GS. Structural biology of the fibres of the collagenous and elastic systems. Cell Biology International. 1996;**20**(1):15-27

[27] Baldock C, Koster AJ, Ziese U, Rock MJ, Sherratt MJ, Kadler KE, et al. The supramolecular organization of fibrillin-rich microfibrils. The Journal of Cell Biology. 2001;**152** (5, 5):1045-1056

[28] Chapman SL, Sicot F-X, Davis EC, Huang J, Sasaki T, Chu M-L, et al. Fibulin-2 and fibulin-5 cooperatively function to form the internal elastic lamina and protect from vascular injury. Arteriosclerosis, Thrombosis, and Vascular Biology. 2010;**30**(1):68-74

[29] Albert EN. Developing elastic tissue. An electron microscopic study. The American Journal of Pathology. 1972;**69**(1):89-102

[30] Wise SG, Weiss AS. Tropoelastin. The International Journal of Biochemistry & Cell Biology. 2009;**41**(3):494-497

[31] Mecham RP. Elastin synthesis and fiber assembly. Annals of the New York Academy of Sciences. 1991;**624**(1):137-146

[32] Rosenbloom J, Abrams WR, Mecham R. Extracellular matrix 4: The elastic fiber. The FASEB Journal. 1993;**7**(13):1208-1218

[33] Mecham RP, Heuser J. Three-dimensional organization of extracellular matrix in elastic cartilage as viewed by quick freeze, deep etch electron microscopy. Connective Tissue Research. 1990;**24**(2):83-93

[34] Cotta-Pereira G, Guerra Rodrigo F, Bittencourt-Sampaio S. Oxytalan, elaunin, and elastic fibers in the human skin. The Journal of Investigative Dermatology. 1976;**66**(3):143-148

[35] Muiznieks LD, Keeley FW. Molecular assembly and mechanical properties of the extracellular matrix: A fibrous protein perspective. Biochimica et Biophysica Acta. 2013;**1832**(7):866-875

[36] Holst J, Watson S, Lord MS, Eamegdool SS, Bax DV, Nivison-Smith LB, et al. Substrate elasticity provides mechanical signals for the expansion of hemopoietic stem and progenitor cells. Nature Biotechnology. 2010;**28**(10):1123-1128

[37] Baldock C, Oberhauser AF, Ma L, Lammie D, Siegler V, Mithieux SM, et al. Shape of tropoelastin, the highly extensible protein that controls human tissue elasticity. Proceedings of the National Academy of Sciences of the United States of America. 2011;**108**(11):4322-4327

[38] Kielty CM, Sherratt MJ, Marson A, Baldock C. Fibrillin microfibrils. In: Anfinsen CB, Edsall JT, Richards FM, Eisenberg DS, editors. Advances in Protein Chemistry. New York: Academic Press; 2005. pp. 405-436

[39] Flory PJ. Crystallinity and dimensional changes in fibrous proteins. Journal of Cellular Physiology. Supplement. 1957;**49**(Suppl 1):175-183

[40] Indik Z, Yeh H, Ornstein-Goldstein N, Kucich U, Abrams W, Rosenbloom JC, et al. Structure of the elastin gene and alternative splicing of elastin mRNA: Implications for human disease. American Journal of Medical Genetics. 1989;**34**(1):81-90

[41] Bashir MM, Indik Z, Yeh H, Ornstein-Goldstein N, Rosenbloom JC, Abrams W, et al. Characterization of the complete human elastin gene. Delineation of unusual features in the 5′-flanking region. The Journal of Biological Chemistry. 1989;**264**(15):8887-8891

[42] Cleary EG, Sandberg LB, Jackson DS. The changes in chemical composition during development of the bovine nuchal ligament. The Journal of Cell Biology. 1967;**33**(3):469-479

[43] Shapiro SD, Endicott SK, Province MA, Pierce JA, Campbell EJ. Marked longevity of human lung parenchymal elastic fibers deduced from prevalence of D-aspartate and nuclear weapons-related radiocarbon. The Journal of Clinical Investigation. 1991;**87**(5): 1828-1834

[44] Watson RE, Griffiths CE, Craven NM, Shuttleworth CA, Kielty CM. Fibrillin-rich microfibrils are reduced in photoaged skin. Distribution at the dermal-epidermal junction. The Journal of Investigative Dermatology. 1999;**112**(5):782-787

[45] Riches K, Angelini TG, Mudhar GS, Kaye J, Clark E, Bailey MA, et al. Exploring smooth muscle phenotype and function in a bioreactor model of abdominal aortic aneurysm. Journal of Translational Medicine. 2013;**11**(1):1-13

[46] Sandberg LB, Soskel NT, Leslie JG. Elastin structure, biosynthesis, and relation to disease states. The New England Journal of Medicine. 1981;**304**(10):566-579

[47] Hasham SN, Willing MC, Guo D, Muilenburg A, He R, Tran VT, et al. Mapping a locus for familial thoracic aortic aneurysms and dissections (TAAD2) to 3p24-25. Circulation. 2003;**107**(25):3184-3190

[48] Robinson PN, Arteaga-Solis E, Baldock C, Collod-Béroud G, Booms P, De Paepe A, et al. The molecular genetics of Marfan syndrome and related disorders. Journal of Medical Genetics. 2006;**43**(10):769-787

[49] Danielson KG, Baribault H, Holmes DF, Graham H, Kadler KE, Iozzo RV. Targeted disruption of decorin leads to abnormal collagen fibril morphology and skin fragility. The Journal of Cell Biology. 1997;**136**(3):729-743

[50] Nikolovska K, Renke JK, Jungmann O, Grobe K, Iozzo RV, Zamfir AD, et al. A decorin-deficient matrix affects skin chondroitin/dermatan sulfate levels and keratinocyte function. Matrix Biology. 2014;**35**:91-102

[51] Stephens EH, Saltarrelli JG, Baggett LS, Nandi I, Kuo JJ, Davis AR, et al. Differential proteoglycan and hyaluronan distribution in calcified aortic valves. Cardiovascular Pathology. 2011;**20**(6):334-342

[52] Tan HT, Lim TK, Richards AM, Kofidis T, Teoh KL-K, Ling LH, et al. Unravelling the proteome of degenerative human mitral valves. Proteomics. 2015;**15**(17):2934-2944

[53] Park PW. Isolation and functional analysis of syndecans. Methods in Cell Biology. 2018;**143**:317-333

[54] Latif N, Sarathchandra P, Taylor PM, Antoniw J, Yacoub MH. Molecules mediating cell-ECM and cell-cell communication in human heart valves. Cell Biochemistry and Biophysics. 2005;**43**(2):275-287

[55] Balaoing LR, Post AD, Lin AY, Tseng H, Moake JL, Grande-Allen KJ. Laminin peptide-immobilized hydrogels modulate valve endothelial cell hemostatic regulation. PLoS One. 2015;**10**(6):e0130749

[56] Robinson CR, Roberts WC. Outcome of combined mitral and aortic valve replacement in adults with mucopolysaccharidosis (the Hurler syndrome). The American Journal of Cardiology. 2017;**120**(11):2113-2118

[57] Pierce OM, McNair GR, He X, Kajiura H, Fujiyama K, Kermode AR. N-glycan structures and downstream mannose-phosphorylation of plant recombinant human alpha-L-iduronidase: Toward development of enzyme replacement therapy for mucopolysaccharidosis I. Plant Molecular Biology. 2017;**95**(6):593-606

[58] Braunlin E, Steinberger J, DeFor T, Orchard P, Kelly AS. Metabolic syndrome and cardiovascular risk factors after hematopoietic cell transplantation in severe mucopolysaccharidosis type I (Hurler syndrome). Biology of Blood and Marrow Transplantation. 2018. pii: S1083-8791(18)30044-2. DOI: 10.1016/j.bbmt.2018.01.028. [Epub ahead of print]

[59] Eisengart JB, Rudser KD, Xue Y, Orchard P, Miller W, Lund T, et al. Long-term outcomes of systemic therapies for Hurler syndrome: An international multicenter comparison. Genetics in Medicine. 2018. DOI: 10.1038/gim.2018.29. [Epub ahead of print]

[60] Sestito S, Falvo F, Scozzafava C, Apa R, Pensabene L, Bonapace G, Moricca MT, Concolino D. Genetics and Gene Therapy in Hunter Disease. Current Gene Therapy. 2018;**18**(2):90-95

[61] Chlebowski MM, Heese BA, Malloy-Walton LE. Early childhood onset of high-grade atrioventricular block in hunter syndrome. Cardiology in the Young. 2018:**28**(5):786-787

[62] Stapleton M, Kubaski F, Mason RW, Yabe H, Suzuki Y, Orii KE, et al. Presentation and treatments for mucopolysaccharidosis type II (MPS II; Hunter syndrome). Expert Opinion on Orphan Drugs. 2017;**5**(4):295-307

[63] Tovar AMF, de Mattos DA, Stelling MP, Sarcinelli-Luz BSL, Nazareth RA, Mourão PAS. Dermatan sulfate is the predominant antithrombotic glycosaminoglycan in vessel walls: Implications for a possible physiological function of heparin cofactor II. Biochimica et Biophysica Acta. 2005;**1740**(1):45-53

[64] Schoen FJ. Future directions in tissue heart valves: Impact of recent insights from biology and pathology. The Journal of Heart Valve Disease. 1999;**8**(4):350-358

[65] Korossis SA, Booth C, Wilcox HE, Watterson KG, Kearney JN, Fisher J, et al. Tissue engineering of cardiac valve prostheses II: Biomechanical characterization of decellularized porcine aortic heart valves. The Journal of Heart Valve Disease. 2002;**11**(4):463-471

[66] Booth C, Korossis SA, Wilcox HE, Watterson KG, Kearney JN, Fisher J, et al. Tissue engineering of cardiac valve protheses I: Development and histological characterization of an acellular porcine scaffold. The Journal of Heart Valve Disease. 2002;**11**(4):457-462

[67] Korossis SA, Wilcox HE, Watterson KG, Kearney JN, Ingham E, Fisher J. In-vitro assessment of the functional performance of the decellularized intact porcine aortic root. The Journal of Heart Valve Disease. 2005;**14**(3):408-421. discussion 422

[68] Granados M, Morticelli L, Andriopoulou S, Kalozoumis P, Pflaum M, Iablonskii P, et al. Development and characterization of a porcine mitral valve scaffold for tissue engineering. Journal of Cardiovascular Translational Research. 2017;**10**(4):374-390

[69] Schoen FJ. Aortic valve structure-function correlations: Role of elastic fibers no longer a stretch of the imagination. The Journal of Heart Valve Disease. 1997;**6**(1):1-6

[70] Morticelli L, Thomas D, Roberts N, Ingham E, Korossis S. Investigation of the suitability of decellularized porcine pericardium in mitral valve reconstruction. The Journal of Heart Valve Disease. 2013;**22**(3):340-353

[71] Luo J, Korossis SA, Wilshaw S-P, Jennings LM, Fisher J, Ingham E. Development and characterization of acellular porcine pulmonary valve scaffolds for tissue engineering. Tissue Engineering Parts A. 2014;**20**:21-22

[72] McCarthy KP, Ring L, Rana BS. Anatomy of the mitral valve: Understanding the mitral valve complex in mitral regurgitation. European Journal of Echocardiography. 2010;**11**(10):i3-i9

[73] Stella JA, Sacks MS. On the biaxial mechanical properties of the layers of the aortic valve leaflet. Journal of Biomechanical Engineering. 2007;**129**(5):757-766

[74] Wang L, Korossis S, Ingham E, Fisher J, JZ. Computational simulation of oxygen diffusion in aortic valve leaflet for tissue engineering applications. The Journal of Heart Valve Disease. 2008;**17**(6):700-709

[75] Ayoub S, Ferrari G, Gorman RC, Gorman JH, Schoen FJ, Sacks MS. Heart valve biomechanics and underlying Mechanobiology. Comprehensive Physiology. 2016;**6**(4):1743-1780

[76] White JF, Werkmeister JA, Hilbert SL, Ramshaw JAM. Heart valve collagens: Cross-species comparison using immunohistological methods. The Journal of Heart Valve Disease. 2010;**19**(6):766-771

[77] Cole WG, Chan D, Hickey AJ, Wilcken DE. Collagen composition of normal and myxomatous human mitral heart valves. Biochemical Journal. 1984;**219**(2):451-460

[78] Lis Y, Burleigh MC, Parker DJ, Child AH, Hogg J, Davies MJ. Biochemical characterization of individual normal, floppy and rheumatic human mitral valves. Biochemical Journal. 1987;**244**(3):597-603

[79] Vafaee T, Thomas D, Desai A, Jennings LM, Berry H, Rooney P, et al. Decellularization of human donor aortic and pulmonary valved conduits using low concentration sodium dodecyl sulfate. Journal of Tissue Engineering and Regenerative Medicine. 2018;**12**(2):e841-e853

[80] Schoen FJ. Evolving concepts of cardiac valve dynamics: The continuum of development, functional structure, pathobiology, and tissue engineering. Circulation. 2008;**118**(18):1864-1880

[81] Bashey RI, Torii S, Angrist A. Age-related collagen and elastin content of human heart valves. Journal of Gerontology. 1967;**22**(2):203-208

[82] Vesely I. The role of elastin in aortic valve mechanics. Journal of Biomechanics. 1997;**31**(2):115-123

[83] Bashey RI, Bashey HM, Jimenez SA. Characterization of pepsin-solubilized bovine heart-valve collagen. Biochemical Journal. 1978;**173**(3):885-894

[84] Grande-Allen KJ, Osman N, Ballinger ML, Dadlani H, Marasco S, Little PJ. Glycosaminoglycan synthesis and structure as targets for the prevention of calcific aortic valve disease. Cardiovascular Research. 2007;**76**(1):19-28

[85] Grande-Allen KJ, Calabro A, Gupta V, Wight TN, Hascall VC, Vesely I. Glycosaminoglycans and proteoglycans in normal mitral valve leaflets and chordae: Association with regions of tensile and compressive loading. Glycobiology. 2004;**14**(7):621-633

[86] Grande-Allen KJ, Griffin BP, Ratliff NB, Cosgrove DM, Vesely I. Glycosaminoglycan profiles of myxomatous mitral leaflets and chordae parallel the severity of mechanical alterations. Journal of the American College of Cardiology. 2003;**42**(2):271-277

[87] Pollock CM, Shadwick RE. Relationship between body mass and biomechanical properties of limb tendons in adult mammals. The American Journal of Physiology. 1994;**266** (3 Pt 2):R1016-R1021

[88] Gosline J, Lillie M, Carrington E, Guerette P, Ortlepp C, Savage K. Elastic proteins: Biological roles and mechanical properties. Philosophical Transactions of the Royal Society of London. Series B, Biological Sciences. 2002;**357**(1418):121-132

[89] Broom ND. The stress/strain and fatigue behaviour of glutaraldehyde preserved heart-valve tissue. Journal of Biomechanics. 1977;**10**(11/12):707-724

[90] Liu J, Qi H. Dissipated energy function, hysteresis and precondition of a viscoelastic solid model. Nonlinear Analysis: Real World Applications. 2010;**11**(2):907-912

[91] Green EM, Mansfield JC, Bell JS, Winlove CP. The structure and micromechanics of elastic tissue. Interface Focus. 2014;**4**(2):20130058

[92] Flügge W. Viscoelasticity. Berlin, Heidelberg: Springer; 1975

[93] Korossis SA, Fisher J, Ingham E. Cardiac valve replacement: A bioengineering approach. Bio-medical Materials and Engineering. 2000;**10**(2):83-124

[94] Nkomo VT, Gardin JM, Skelton TN, Gottdiener JS, Scott CG, Enriquez-Sarano M. Burden of valvular heart diseases: A population-based study. Lancet (London, England). 2006;**368**(9540):1005-1011

[95] Lloyd-Jones D, Adams RJ, Brown TM, Carnethon M, Dai S, De Simone G, et al. Heart disease and stroke statistics—2010 update: A report from the American Heart Association. Circulation. 2010;**121**(7):e46-e215

[96] Chehab G, Saliba Z, El-Rassi I. The silent patent ductus arteriosus. Le Journal Médical Libanais; **56**(1):7-10

[97] Hoffman JI. The global burden of congenital heart disease. Cardiovascular Journal of Africa. 2013;**24**(4):141-145

[98] Hinton RB, Lincoln J, Deutsch GH, Osinska H, Manning PB, Benson DW, et al. Extracellular matrix remodeling and organization in developing and diseased aortic valves. Circulation Research. 2006;**98**(11):1431-1438

[99] Milewicz DM, Dietz HC, Miller DC. Treatment of aortic disease in patients with Marfan syndrome. Circulation. 2005;**111**(11):e150-e157

[100] Pasipoularides A. Calcific aortic valve disease: Part 1—Molecular pathogenetic aspects, hemodynamics, and adaptive feedbacks. Journal of Cardiovascular Translational Research. 2016;**9**(2):102-118

[101] Garg V, Muth AN, Ransom JF, Schluterman MK, Barnes R, King IN, et al. Mutations in NOTCH1 cause aortic valve disease. Nature. 2005;**437**(7056):270-274

[102] Miller JD, Weiss RM, Heistad DD. Calcific aortic valve stenosis: Methods, models, and mechanisms. Circulation Research. 2011;**108**(11):1392-1412

[103] Walker GA, Masters KS, Shah DN, Anseth KS, Leinwand LA. Valvular myofibroblast activation by transforming growth factor-beta: Implications for pathological extracellular matrix remodeling in heart valve disease. Circulation Research. 2004;**95**(3):253-260

[104] Brooke BS, Karnik SK, Li DY. Extracellular matrix in vascular morphogenesis and disease: Structure versus signal. Trends in Cell Biology. 2003;**13**(1):51-56

[105] Pasipoularides A. Calcific aortic valve disease: Part 2—Morphomechanical abnormalities, gene reexpression, and gender effects on ventricular hypertrophy and its reversibility. Journal of Cardiovascular Translational Research. 2016;**9**(4):374-399

[106] Weiss RM, Miller JD, Heistad DD. Fibrocalcific aortic valve disease: Opportunity to understand disease mechanisms using mouse models. Circulation Research. 2013;**113**(2):209-222

[107] Conti CA, Della Corte A, Votta E, Del Viscovo L, Bancone C, De Santo LS, et al. Biomechanical implications of the congenital bicuspid aortic valve: A finite element study of aortic root function from in vivo data. The Journal of Thoracic and Cardiovascular Surgery. 2010;**140**(4):890-896

[108] Konduri S, Xing Y, Warnock JN, He Z, Yoganathan AP. Normal physiological conditions maintain the biological characteristics of porcine aortic heart valves: An ex vivo organ culture study. Annals of Biomedical Engineering. 2005;**33**(9):1158-1166

[109] Balachandran K, Konduri S, Sucosky P, Jo H, Yoganathan AP. An ex vivo study of the biological properties of porcine aortic valves in response to circumferential cyclic stretch. Annals of Biomedical Engineering. 2006;**34**(11):1655-1665

[110] Quick DW, Kunzelman KS, Kneebone JM, Cochran RP. Collagen synthesis is upregulated in mitral valves subjected to altered stress. ASAIO Journal; **43**(3):181-186

[111] Balachandran K, Alford PW, Wylie-Sears J, Goss JA, Grosberg A, Bischoff J, et al. Cyclic strain induces dual-mode endothelial-mesenchymal transformation of the cardiac valve. Proceedings of the National Academy of Sciences of the United States of America. 2011;**108**(50):19943-19948

[112] Rajamannan NM, Subramaniam M, Rickard D, Stock SR, Donovan J, Springett M, et al. Human aortic valve calcification is associated with an osteoblast phenotype. Circulation. 2003;**107**(17):2181-2184

[113] Leopold JA. Cellular mechanisms of aortic valve calcification. Circulation. Cardiovascular Interventions. 2012;**5**(4):605-614

[114] Zhiduleva EV, Irtyuga OB, Shishkova AA, Ignat'eva EV, Kostina AS, Levchuk KA, et al. Cellular mechanisms of aortic valve calcification. Bulletin of Experimental Biology and Medicine. 2018;**164**(3):371-375

[115] Gharacholou SM, Karon BL, Shub C, Pellikka PA. Aortic valve sclerosis and clinical outcomes: Moving toward a definition. The American Journal of Medicine. 2011;**124**(2):103-110

[116] Owens DS, Otto CM. Is it time for a new paradigm in calcific aortic valve disease? JACC. Cardiovascular Imaging. 2009 Aug;**2**(8):928-930

[117] Thubrikar MJ, Aouad J, Nolan SP. Patterns of calcific deposits in operatively excised stenotic or purely regurgitant aortic valves and their relation to mechanical stress. The American Journal of Cardiology. 1986;**58**(3):304-308

[118] Lindman BR, Clavel M-A, Mathieu P, Iung B, Lancellotti P, Otto CM, et al. Calcific aortic stenosis. Nature Reviews Disease Primers. 2016;**2**:16006

[119] Dai G, Kaazempur-Mofrad MR, Natarajan S, Zhang Y, Vaughn S, Blackman BR, et al. Distinct endothelial phenotypes evoked by arterial waveforms derived from atherosclerosis-susceptible and -resistant regions of human vasculature. Proceedings of the National Academy of Sciences of the United States of America. 2004;**101**(41):14871-14876

[120] Otto CM. Calcific aortic stenosis--time to look more closely at the valve. The New England Journal of Medicine. 2008;**359**(13):1395-1398

[121] Parmar KM, Larman HB, Dai G, Zhang Y, Wang ET, Moorthy SN, et al. Integration of flow-dependent endothelial phenotypes by Kruppel-like factor 2. The Journal of Clinical Investigation. 2006;**116**(1):49-58

[122] Cosgrove DM, Stewart WJ. Mitral valvuloplasty. Current Problems in Cardiology. 1989;**14**(7):359-415

[123] Whittaker P, Boughner DR, Perkins DG, Canham PB. Quantitative structural analysis of collagen in chordae tendineae and its relation to floppy mitral valves and proteoglycan infiltration. British Heart Journal. 1987;**57**(3):264-269

[124] Rabkin E, Aikawa M, Stone JR, Fukumoto Y, Libby P, Schoen FJ. Activated interstitial myofibroblasts express catabolic enzymes and mediate matrix remodeling in myxomatous heart valves. Circulation. 2001;**104**(21):2525-2532

[125] Barber JE, Kasper FK, Ratliff NB, Cosgrove DM, Griffin BP, Vesely I. Mechanical properties of myxomatous mitral valves. The Journal of Thoracic and Cardiovascular Surgery. 2001;**122**(5):955-962

[126] Barber JE, Ratliff NB, Cosgrove DM, Griffin BP, Vesely I. Myxomatous mitral valve chordae. I: Mechanical properties. The Journal of Heart Valve Disease. 2001;**10**(3):320-324

[127] Gupta V, Werdenberg JA, Blevins TL, Grande-Allen KJ. Synthesis of glycosaminoglycans in differently loaded regions of collagen gels seeded with valvular interstitial cells. Tissue Engineering. 2007;**13**(1):41-49

[128] Gupta V, Werdenberg JA, Lawrence BD, Mendez JS, Stephens EH, Grande-Allen KJ. Reversible secretion of glycosaminoglycans and proteoglycans by cyclically stretched valvular cells in 3D culture. Annals of Biomedical Engineering. 2008;**36**(7):1092-1103

[129] Combs MD, Yutzey KE. Heart valve development: Regulatory networks in development and disease. Circulation Research. 2009;**105**(5):408-421

[130] Sainger R, Grau JB, Branchetti E, Poggio P, Seefried WF, Field BC, et al. Human myxomatous mitral valve prolapse: Role of bone morphogenetic protein 4 in valvular interstitial cell activation. Journal of Cellular Physiology. 2012;**227**(6):2595-2604

[131] Mohler ER, Gannon F, Reynolds C, Zimmerman R, Keane MG, Kaplan FS. Bone formation and inflammation in cardiac valves. Circulation. 2001;**103**(11):1522-1528

[132] Pflaum M, Kühn-Kauffeldt M, Schmeckebier S, Dipresa D, Chauhan K, Wiegmann B, et al. Endothelialization and characterization of titanium dioxide-coated gas-exchange membranes for application in the bioartificial lung. Acta Biomater. 2017;**50**:510-21

IntechOpen